Shouzhuang Li

PET recycling via gasification - Influence of operating conditions on product distribution

School of Engineering

Master's thesis

Espoo 26.06.2019

Supervisor:	Mika Järvinen,	Aalto University, Finland
Advisors:	Isabel Cañete Vela,	Chalmers University of Technology, Sweden

Aalto University
School of Engineering

Aalto University, P.O. BOX 11000, 00076
AALTO
www.aalto.fi
Abstract of the master's thesis

Author Shouzhuang Li

Title PET recycling via gasification - Influence of operating conditions on product distribution

Degree programme Nordic Master Programme in Innovative Sustainable Energy Engineering

Major Innovative Sustainable Energy Engineering **Code of major** ENG215

Teacher in charge Mika Järvinen

Advisors Isabel Cañete Vela

Date 26.06.2019 **Number of pages** 72+12 **Language** English

Abstract

EU plans to achieve 100% plastic packaging reuse in 2040, and some new technologies have been proposed. Gasification is one of the promising technologies to convert plastic into syngas for heat production or chemicals synthesis process. This project focused on the thermoplastic that is widely used in textile fibre, film, and bottles – PET. Although PET bottle recycling is reliable, gasification could be an option for recycling contaminated and other PET products.

Proximate analysis was carried out by Thermogravimetric Analysis (TGA) to comprehend its thermal decomposition, obtaining volatiles and char. Gasification experiments were conducted in a lab scale bubbling fluidized bed with batch and continuous feeding operation. The batch experiments compared different plastics and gasifying agents. It was found that CO_2 dominated the gas production at all agents, and steam can motivate H_2 production. However, air cannot reduce tar formation significantly as literature stated. After that, continuous feeding experiments for steam gasification were designed to investigate how temperature, residence time and steam/fuel ratio affect the distribution of gas and tar products in PET steam gasification. The results show the temperature is an essential condition parameter for gas and tar yield. The increasing temperature improved the gas yield and tar cracking.

The application of syngas produced by PET steam gasification was evaluated based on the experimental results. The highest energy conversion efficiency from PET and reacted steam to cold syngas was 29% at 800 °C, meaning that most of heat energy was lost. Fuel synthesis was analyzed by H_2/CO ratio, and syngas products are more likely to be produced fuels by FT synthesis. Besides, the tar limitation of both power generation and fuel synthesis are very strict, but the tar concentrations in all cases are extremely high. Mixing with other plastics or biomass and better bed material could be solutions to promote syngas quality. Moreover, the mass balance analysis suggests 35% - 40% carbon was not detected, so sampling and measurement methods should be improved in the future research.

Keywords PET, Steam gasification, Bubbling fluidized bed, Heat production, Fuel synthesis

Acknowledgements

I am heartily thankful to my supervisor, Isabel Cañete Vela, who guided me patiently and cared so much about my work throughout the thesis work. Your advice and encouragement improved me a lot. Further, I would like to thank my examiner, Martin Seemann, for providing the opportunity to do the master thesis on the topic of PET gasification, and the valuable comments on planning report and thesis. Moreover, I appreciate I had an opportunity to attend the Swedish Gasification Centre (SFC) conference in April, where I learnt a lot and gained fresh ideas for my thesis.

Also, I am indebted to the participants in the experimental work: Jessica Bohwalli and Javier Calvo. With your help, my experiments and thesis went smoothly. To Jessica, thank you for your work in SPA product analysis and TGA. To Javier Calvo, thanks for assisting in bubbling fluidized bed experiments.

I am grateful to my friends Daofan Cao and Zhaoyang Fan, who aided me to finish the SPA results analysis with their knowledge and skills. Otherwise, I would have had a tough time in the data analysis.

I would thank all the friends I meet in the thesis office, we helped and encouraged each other. Also, the Division of Energy Technology provides a comfortable work environment for us. I enjoyed every moment I spent in the Division of Energy Technology, especially every Friday's fika.

Last but not least, heartfelt thanks go to my parents. Words can not express how grateful I am to you because you are the most important people in my world. With your emotional support, I do not feel lonely when I study abroad.

Shouzhuang Li, Gothenburg, June 2019

Contents

List of Figures

List of Tables

Nomenclature

Abbreviations

μ-GC	Micro Gas Chromatography
BHET	Bis-(2-hydroxyethyl) Terephthalate
DME	Dimetylester
DMT)	Dimethyl Terephthalate
DTG	Derivative of Thermogravimetric
EG	Ethylene Glycol
ER	Equivalence Ratio
FID	Flame Ionzation Detector
FT-IR	Fourier-transform Infrared Spectroscopy
FTS	Fischer-Tropsch Synthesis
GC/MS	Gas Chromatography–Mass Spectrometry
HDPE	High Density Polyethylene
LDPE	Low Density Polyethylene
PE	Polyethylene
PET	Polyethylene Terephthalate
PP	Polypropylene
PS	Polystyrene
PSW	Plastic Solid Waste
PU	Polyurethanes
PVC	Polyvinyl Chloride
SF	Steam to Fuel ratio
SNG	Synthesis Natural Gas
SPA	Solid-Phase Adsorption
SPI	Society of the Plastics Industry
TDH	Transport Disengaging Height
TGA	Thermogravimetric Analysis
TPA	Terephthalic Acid
WGS	Water-gas Shift

Greek Symbols

α	Gas Volmetric Percentage	
$\bar{\mu}$	The mean of a series of data	
δ	The improvement factor	
ϵ_{mf}	The porosity of the bed at the state of minimum fluidization	
μ	Dynamic viscosity of gas	Pa/s
ψ	Sphericity of particles	
ρ	Gas density	g/L

ρ_b	Bulk density of the bed material	kg/m^3
ρ_c	Density of particles	kg/m^3
ρ_g	Density of gas	kg/m^3
σ	Standard deviation	
τ	Residence time	s

Other Symbols

$\bar{M}$	The molar mass	g/mol
$\dot{m}_{steam,190°C}$	Steam mass flow rate at 190 $°C$	g/min
$\dot{V}_{20°C}$	Gas volumetric flow rate at 20 $°C$	l/min
A	The cross-section area of the bed	m^2
$Area\%$	The area percentage read from GC results	
C_v	Coefficient of variation	
d_p	Average diameter of particles	m
f	The mass fraction of VPET in the mixture of VPET and bed material	
H	The bed height after expansion	m
H_f	The bed height of fixed bed	m
H_{mf}	The bed height at minimum fludization state	m
H_{MP5}	The height of measurement point MP5	cm
M	Mass of bed material	kg
$m_{feedstock}$	The mass of plastics	g
$m_{standard}$	The mass standard solution	μg
n	Molar gas yield	mol/kg
U	Superficial velocity	m/s
U_{mb}	Minimum bubbling velocity	m/s
U_{mf}	Minimum fluidization velocity	m/s
$wt\%$	The weight fraction from TGA proximate analysis result	

1

Introduction

1.1 Background

Plastics play a crucial role in the modern style of living and deliver a sustainable future. It is an essential material in many sectors, such as packaging, construction, agriculture, households, medical and other applications due to their properties of resistance to corrosion, low density and durability [1] [2]. In 2017, the production of plastic reached 348 million tonnes all over the world. In plastic's family, thermoplastic is the most commonly used, including polyethylene (PE), polypropylene (PP), polyethylene terephthalate (PET), polyvinyl chloride (PVC), polystyrene (PS), and Polyurethanes (PU). The share of different types of thermoplastic demand in Europe in 2017 is shown in Figure 1.1. PE represented the highest consumption, around 30%. The second largest group was PP (19.3%), followed by PVC, PUR, PET, and PS (around or smaller than 10%) [3].

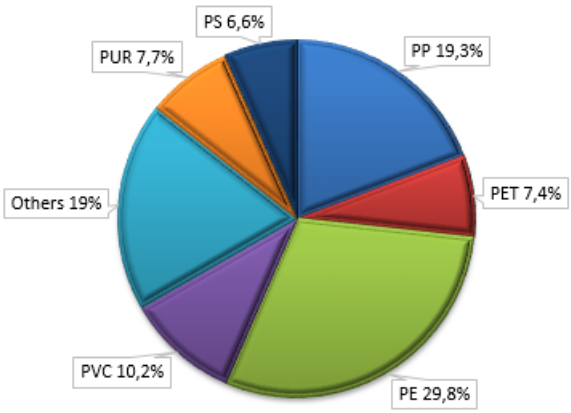

Figure 1.1: European plastic converter demand by polymer types in 2017 [3]

However, waste management becomes a severe problem with the significant surge of plastic. Figure 1.2 illustrates global plastic production and management between 1950 and 2015 globally [4]. In the cumulative plastic solid waste (PSW) in 65 years, only 800Mt (12%) and 600Mt (9%) have been incinerated and recycled respectively, while nearly 60% of PSW was left in the landfills or natural environment.

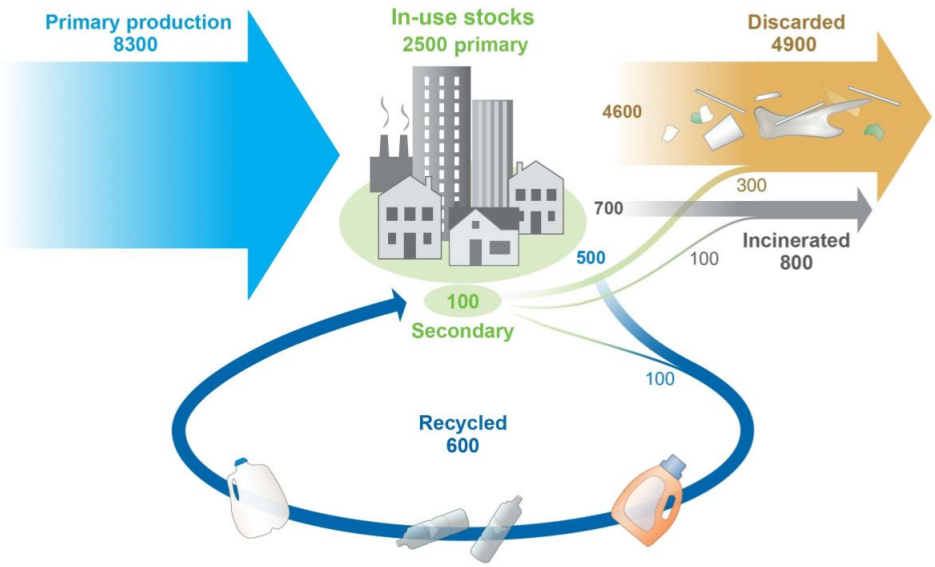

Figure 1.2: Global plastic production and management from 1950 to 2015. [4]

Due to the low degradability, the PSW can remain in the soil semi-permanently, which can result in soil contamination and reduce the capacity for waste landfills. Therefore, alternative options of PSW management have to be proposed. Besides, since plastics are derived from fossil fuel, they have the potential to be converted into energy,fuels and other products.

Among the thermoplastics, PET is the most favorable food packaging material, mainly for soft drinks and mineral water, because of its light weight and large containing capacity [6]. Although PET bottles are recycled nowadays, PET is also widely used in the electrical and electronic industry, automotive industry and textile industry. The continuous rising of PET utilization facilitates the research of its recycling. Thus, in this thesis, PET will be the research object.Recently, given the operational and environmental advantages, chemical recycling has gained more attention, as a method of producing various fuels by the process of thermolysis [5]. Pyrolysis and gasification are the two main thermolysis processes.

Pyrolysis is the process that is degrading the long chain polymer into smaller molecules with intense heat and the absence of oxygen [6]. However, PET is not recommended for pyrolysis because the majority of products are gas with low oil yield. Besides, the terephthallic acid and/or similar products will condensate to solid phase when cooled, which can clog up pipes [7].

If pyrolysis is not suitable for PET, gasification can be another solution. The objective of gasification is to convert carbonaceous materials into gaseous products (e.g.,

the mixture of H_2, CO, CH_4 and CO_2). In comparison to incineration and pyrolysis, in the gasification process, the oxidizing agent is introduced into the system in sub-stoichiometric quantities, and PET is partially oxidized into CO and H_2 at the temperature range of 550–1000°C [8]. A remarkable advantage is that gasification is more flexible to treat various composites of feedstocks. Plus, gasification can be integrated into current energy systems, such as heat generation and fuel production, so, it is promising and attractive [1] [9]. A large amount of research about biomass and coal has been carried out and, by the end of 2016, there were around 1,014 gasification projects with around 2559 gasifiers worldwide [10]. These successful examples and mature technologies provide valuable experience for the application of gasification to PET recycling.

Nevertheless, the reaction mechanisms and gasifier design of plastic gasification are not the same as for biomass and coal due to the special features: (1) low thermal conductivity; (2) sticky behavior; (3) high volatile content and (4) notable tar formation [1]. Researchers focused more on PE, PP, and their co-gasification with biomass or coal, but so far, PET gasification has been seldom carried out. Therefore, PET gasification will be the topic of this thesis.

1.2 Aim of the thesis

The objective of this thesis is to investigate the influence of operation conditions on the PET gasification product distribution in a laboratory scale fluidized bed. Some questions must be answered step by step to achieve this goal.

1. *How much moisture, volatiles, char and ash does PET contain?* The proximate analysis, in which char content is essential for gasification reactions, and the thermal decomposition can influence the operation conditions of the process. This was carried out by thermogravimetric analysis (TGA).

2. *Which gasifying agent should be chosen to produce high quality syngas?* Air, oxygen, CO_2 and steam can work as medium for gasification process, one of them will be selected for the next experiment to reach high quality syngas production. This experiment is conducted by batch feeding in a lab scale bubbling fludized bed (BFB).

3. *How do the operating conditions affect the gas and tar product distribution, and which condition is the most important?* This is the main aim of this thesis. The most important condition could influence the process notably, which could be used to improve the syngas quality significantly. The feedstock will be fed contiunously

into BFB to guarantee the experiment close to the reality.

4. *What are the feasible applications of the products?* The possibility of PET gasification integrated with heat generation and fuel production was analyzed, and some possible methods were proposed to solve the problems.

2

Theory

This chapter will describe the details of PET thermal chemical decomposition process, for instance, the basic structure of PET, its synthesis process, PET bottle recycling, principles of PET pyrolysis and gasification, bubbling fluidized bed and processes reported in other literatures. This fundamental knowledge is prerequisite for the experimental work and data analysis.

The structure and identification code of PET are illustrated in Figure 2.1. PET is a linear partly aromatic polyester with a repeating unit of $C_{10}H_8O_4$. The repeating part containing an aromatic ring gives the properties of remarkable stiffness and strength. Together with the good resistance of some chemicals(weak acid and organic solvent) and excellent barrier for CO_2, PET becomes a popular choice for food containers, beverage and water bottles. The identification code of PET is number 1.

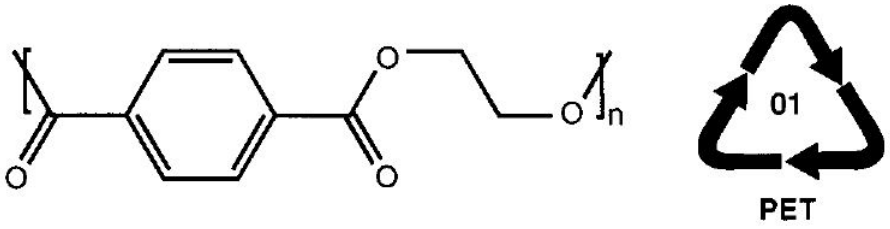

Figure 2.1: The Structure and identification code of PET [11]

2.1 PET production

PET is polymerized by the polycondensation reactions in the presence of a catalyst and stabilizer [13]. The monomer of PET, bis-(2-hydroxyethyl) terephthalate (BHET), can be produced from the ethylene glycol (EG) either esterification with terephthalic acid (TPA) or transesterification with dimethyl terephthalate (DMT) [11]. The two-step synthesis process is depicted in Figure 2.2.

Despite producing the same polymer, the details of two synthesis reaction routes still differ due to different types of reactions and raw materials. The comparison of the two methods is shown in 2.1. Route A (esterification) and Route B (transesterification)

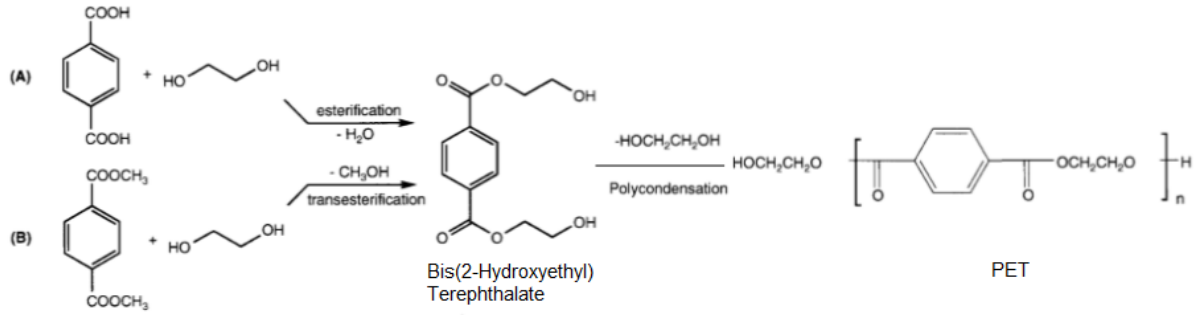

Figure 2.2: Synthesis of PET by direct esterification (A) and transesterification (B) reactions [11]

have similar required temperature. But higher pressure is necessary for Route A while catalyst is significant for Route B. Compared with Route A, a valuable by-product – methanol can be produced in Route B. But too much methanol can slow down the reaction, so a stripping column is designed to remove excess methanol [14].

Table 2.1: The comparison of PET synthesis [14]

	Route A (esterification)	Route B(transesterification)
Temperature	250°C	245°C
Pressure	2.75kPa	Atmospheric
By-products	H_2O	Methanol
Catalyst	No	Zn or Ca salt

After esterification or transesterification process, PET polycondensation is carried out at the temperature of 275°C under vacuum condition (15-100 mmHg) [14]. The most important catalyst is antimony trioxide (Sb_2O_3) that will remain in the products, so about 170-300mg/kg Sb with other metals such as Co, Fe, Mn, and Cr were also detected in PET bottles [16]. Besides, carbonyl compounds like formaldehyde and acetaldehyde can be generated by thermo-mechanical and thermo-oxidative degradation of PET. Plastic bottles (28%) and fibers (68%) [15] are the most common applications of PET. With regard to plastic bottles production, some additives are required. For instance, the addition of plasticizers (phthalates and dipates) can improve the softness and flexibility of bottles. Although PET has good barrier properties, additives e.g. lamellar polyamide and 1,3-benzenedimethanamine(MXD6) are necessary for reducing the permeability of CO_2 and O_2 [16].

2.2 PET recycling

In 2018, 55% global PET resin was recycled [15]. However, for how much PET fibers have been recycled, there is no report. The treatment and recovery process can be allocated into four categories: re-extrusion (primary), mechanical (secondary), chemical (tertiary) and energy recovery (quaternary) [5]. Primary recycling is also known as pre-consumer industrial scrap or (re-extrusion), which recycles the plastic "in-plant" with simplicity and low cost. The recycled scrap or waste is either mixed with virgin material to assure product quality or used as a second-grade material [18]. The mechanical recycling involves sorting, contaminants removal, size reducing, melting, and remolding [19]. However, the viscosity, thermal, and mechanical resistance are likely to decrease. Additionally, other products such as cyclic and linear oligomers can be generated during the melting; both of them will affect the quality of the final products [20].

Apart from pyrolysis and gasification, PET chemical recycling can be carried out by solvolysis. Solvolysis, the reaction in which the solvent is the reactant and solvolytic reactions are always substitution reaction, in the case of PET recycling, including methanolysis, hydrolysis, glycolysis, aminolysis, and others. The aim of solvolysis is to obtain the raw materials for PET production. So it can be seen as the reverse process of the synthesis reactions. High purity PET is required for solvolysis because the impurities in PET can stop the reactions [12, 18–20]. Table 2.2 illustrates different routes of PET solvolysis.

The process of hydrolysis and methanolysis are the solvolysis routes that obtain the monomer of PET production by routes (A) and (B) respectively, and glycolysis can be helpful to produce the oligomer–BHET. These products are mostly used the form of fibres (72%), bottles (10%), sheets (10%), strapping tape (5%) and others (3%) [21]. So far, glycolysis and methanolysis have achieved commercial application [18]. For instance, Far Eastern New Century Co., Ltd. (FENC) runs a small scale glycolysis unit. The process is conducted at the temperature of 180 - 250 °C with the absence of catalysts. BHET is repolymerized to produce PET fibre, and the material conversion efficiency can achieve 96% [21].

Figure 1.2 suggests that incineration was the main plastic recycling method between 1950 to 2015. Plastics are always combusted with other municipal solid wastes to produce heat or electricity, so few applications of PET incineration were reported. However, C.E Komly et al [22] developed a mathematical model to assess the life cycle analysis (LCA) of PET bottles waste management. They calculated that 1 kg PET bottles incineration can produce average of 0.51 kWh of electricity and 4.25 MJ of heat. At the same time, burning 1 kg PET releases 2.3kg CO_2 [23].

Table 2.2: Summary of PET solvolysis routes [18, 19]

	Solvent	Main product	Temperature (°C)	Pressure (MPa)	Reaction time (h)	Conversion efficiency (wt%)
Hydrolysis	4-20wt% $NaOH$or KOH	TPA and EG	210-250	1.4-2	3-5	99
	Concentrated H_2SO_4 (at least 70wt%)		30-100	-	3-72	-
	water		200-300	1-4	-	-
Methanolysis	Methanol	DMT and EG	180-280	2-4	-	-
Glycolysis	glycols	BHET	180-250	-	0.5-8	-
Aminolysis	ammonia	Terephth -alamide	120-180	2	1-7	>90

2.3 PET pyrolysis

The reaction mechanism of PET depolymerization is random scission [1], so the mechanisms of pyrolysis would be very complicated due to the existence of oxygen atom. Many PET cleavage scheme were proposed, most of which were carried out with the help of TGA as well as FT-IR system [29, 30]. One of the most likely thermal cleavage mechanisms of PET pyrolysis is displayed in Figure 2.3.

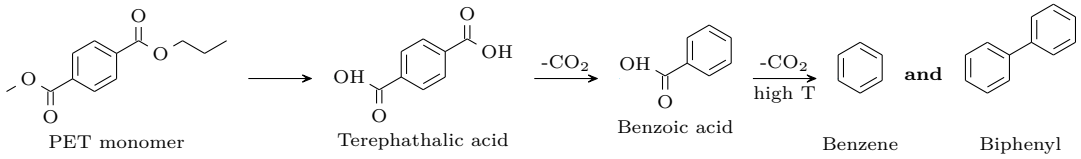

Figure 2.3: One of the most likely thermal cleavage mechanisms of PET pyrolysis [31]

The products of PET pyrolysis can be syngas, tar, and char, and the proportion of them rely on the operating conditions such as temperature, pressure, catalyst and residence time. Usually, the liquid products can be refined to produce petroleum, some PET pyrolysis lab scale experiment are illustrated in Table 2.3.

Fakhr Hoseini & Dastanian studied the pyrolysis of low-density polyethylene (LDPE), PP and PET at 5 different heating rates at the temperature of 500°C. They discovered

Table 2.3: Summary of studies on PET pyrolysis

Reference	Plastic	Reactor	Process parameters		Heating rate	Yield(wt%)		
			Temperature	Pressure	°C/min	Gas	Liquid	Solid
[32]	PET	-	500	1 atm	6	52.13	38.89	8.98
[32]	PET	-	500	1 atm	10	60.23	32.13	7.64
[32]	PET	-	500	1 atm	14	65.12	29.14	5.74
[32]	PP	-	500	1 atm	14	21.74	78.26	0
[32]	LDPE	-	500	1 atm	14	28.85	71.11	0.04
[33]	PET	Fixed Bed	500	-	10	76.9	23.1	-

that PET pyrolysis produced much more gas and solid towards other two plastics and gas yield increased with the rising heating rate [32]. Çepelioğullar & Pütün observed about 76.9% PET was converted into the gas product through pyrolysis [33]. Because PET consumes less energy to convert into other chemicals and the reaction mechanism of pyrolysis is prone to produce gas production [6]. Table 2.4 shows the main products of PET pyrolysis and their weight percentage distribution from different references. Because of different reactors and reaction conditions, the distribution of the products

Table 2.4: Summary of PET pyrolysis main products (wt%)

Reference	[34]	[35]	[34]	[36]
Temperature (°C)	500	510	600	600
CO_2	29.28	13	31.08	20.73(including Acetaldehyde)
CO	9.88	23	14.21	-
H_2	-	0.09	-	-
$Methane$	-	0.87	-	-
$C2$	3.09	1.5	3.35	-
$C3$	0.37	0.71	0.22	-
$C4$	0.16	0.39	0.24	0.28
$Benzene$	1.04	0.58	0.81	2.75
$Toluene$	0.1	-	0.1	0.36
$Acetaldehyde$	11.11	-	11.06	-
$Benzoicacid$	26.98	21	21.91	10.10
$4-[(Vinyloxy)carbonyl]benzoicacid$	-	-	-	27.08
$Benzoylformic$	2.55	-	6.89	-
Other	15.44	38.86	10.13	38.7

varies. [34], [35], [36] were carried out in spouted bed, microfurnace and fluidized bed, respectively. The scale and mechanism of these three reactors were distinct. Temper-

ature is an essential parameter for pyrolysis, which can affect the product distribution noticeably.

2.4 PET gasification

Gasification pursues the maximum of feedstocks to gas products. In general, gasification process can be separated into several steps based on temperature range: (i) drying; (ii) pyrolysis (devolatilization); (iii) Tar cracking, reforming, combustion and shifting depending on the gasifying agent and (iv) char heterogeneous gasification reactions [1, 24–26].

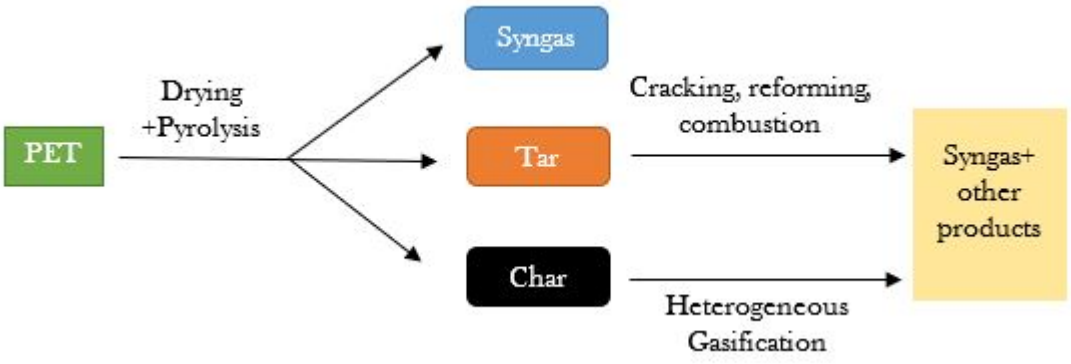

Figure 2.4: Scheme of PET gasification steps

Due to the distinct opinions of the scope of pyrolysis and gasification, researchers have different definitions. To avoid confusion, the concepts used in this thesis must be clarified. Some researchers viewed tar cracking and reforming belonged to pyrolysis step, so some terms like steam pyrolysis were proposed, and some researchers regarded tar cracking and reforming as a part of gasification reactions [25,27,28]. For instance, TGA shows the remaining char of PE and PP pyrolysis is almost zero, and char gasification seldom takes place. In this thesis, since char can be detected from PET pyrolysis, tar cracking and reforming as well as other partial oxidized reactions are considered as step 3 and reactions related to char is the fourth step. In the case of PET, moisture content is very low, which decreases the importance of drying in the gasification process (see in Figure 2.4).

2.4.1 Gasification agent

Gasifying agent (also called gasifying medium) reacts with char and heavier hydrocarbons to convert them into low molecular weight gases [24]. The commonly used gasifying agent includes air, oxygen, steam and CO_2.

Air simplified the whole process, and reduce energy and the cost of production. After pyrolysis step, the partial combustion of hydrocarbons provides heat for the char gasification. It is the same principle when pure oxygen is applied instead of air to increase the amount of CO and CO_2. However, it is costly to separate the air to obtain pure oxygen. Besides, oxygen feeding cannot exceed the stoichiometric amount; otherwise the "fuel gas" will be changed into "flue gas" that is without chemical energy [24]. This fact suggests the equivalence ratio (ER) influences the gas yield and the distribution of gasification products [1].

Introducing steam into the gasifier aims to improve the yield of H_2 However, steam reforming is an endothermic reaction, meaning that higher energy consumption compared to air or oxygen. Therefore, temperature is an essential parameter for steam gasification, and the higher the temperature, the more gas yield and hydrogen production [1].The drawback of steam gasification is generating more tars than air or oxygen.

Similarly, the purpose of gasifying agent CO_2 is to obtain more CO, but has no obvious effect on tar reduction. Most CO_2 gasification analysis was involved in TGA. As for the reactor scale, Saad and William investigated CO_2 gasification of LDPE, HDPE, PS, PET, PP and the mixture for a new solution to CO_2 capture instead of the underground storage. They observed that compared with PET pyrolysis, CO concentration increased but not so rapidly as other plastics when CO_2 was fed, and H_2 and CH_4 correspondingly reduced [37].

2.4.2 Tar reduction

The main challenge of plastic gasification is the formation of tar. The various definitions of tar were given by different researchers, the most common is: The organics produced under thermal or partial-oxidation regimes (gasification) of any organic material are called “tars” and are generally assumed to be mostly aromatic [38]. Tar is a complex mixture of condensable hydrocarbons, oxygen- containing aromatic molecules and others [24]. From Table 2.4, it can be seen that Benzoic acid is one of the most crucial but primary tars at temperatures between 500 and 600 °C. With the increment of temperature and residence time, the primary tar can be converted into secondary and tertiary tars, which are stable and hard to remove, as Figure 2.5 shows [1].

Tar is the by-product of PET gasification, but sometimes it is not desirable. The viscosity of tar is high, clogging the gasifier or pipelines when it is condensed at low temperature. The remained low dew point tar in syngas product can destroy the engine when syngas is fed as fuel gas [24]. Part of tar can be reduced by the gasifying agent in the gasifier, the reactions are described in Table 2.5 [39, 40].

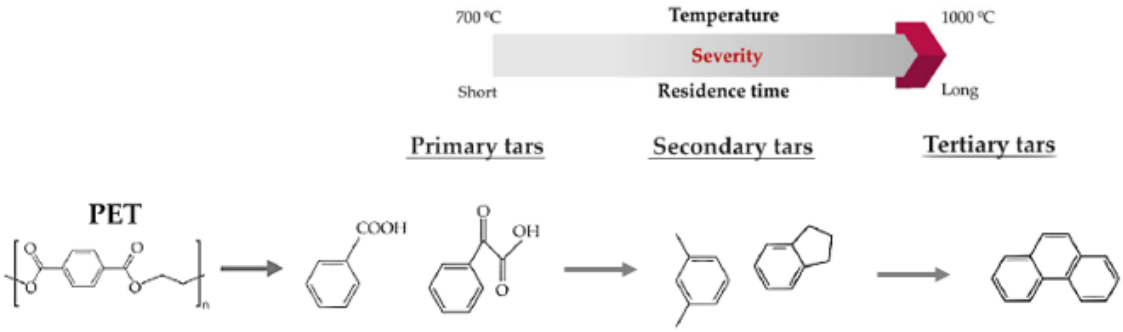

Figure 2.5: Tar formation and evaluation pathways in the gasification of PET [1]

Table 2.5: Main reactions of tar reduction [39, 40]

No.	Reaction type	Reaction	Reaction heat ΔH^0 kJ/mol
R1	Partial oxidation	$CnHm + (n/_2)O_2 \longrightarrow nCO + (m/_2)H_2$	-715 ∼ -2538
R2	Steam reforming	$CnHm + nH_2O \rightleftharpoons (m/_2 + n)H_2 + nCO$	+740 ∼ +2302
R3	Dry reforming	$CnHm + nCO_2 \rightleftharpoons 2\,nCO + (m/_2)H_2$	+980∼ +3112
R4	Thermal cracking	$CnHm \longrightarrow C + CxHy$	-161 ∼ -505
R5	Hydrocracking	$CnHm + H_2 \longrightarrow CxHy$	-498 ∼ -1815

Note: CmHn represents the high molecular weight tars and CxHy stands for lighter tars

Gasifying agents cannot remove all tars because introducing more agent can lead to the low quality of products, as the last part mentioned. Therefore, catalysts and optimized gasifier design would be required. If higher quality syngas is necessary, post-gasification tar removal should be applied [24]. Table 2.6 lists post-gasification tar reduction efficiency. It seems that only catalytic cracking is reliable in all post-gasification tar reduction.

Table 2.6: Post-gasification tar reduction efficiency (%) [41]

Sand bed filter	Wash tower	Venturi scrubber	Wet electrostatic precipitator	Fabric filter	Rotational particle separator	Fixed bed tar adsorber	Catalytic tar cracker
50-97	10-25	50-90	0-60	0-50	30-70	50	> 95

2.4.3 Gasification reactions

Char produced from thermal decomposition is not a pure carbon. It also contains hydrocarbons and other chemicals [24]. Related reactions are illustrated in Table 2.7.

The step of pyrolysis and tar reduction reactions are much more rapid than heterogeneous char gasification. Therefore, steam gasification, boundouard reaction, and hydrogasification reaction are the slowest reactions in gasification process. Both steam gasification and boundouard reaction require heat input, and the reactions would be favored at high temperature. Usually, for steam gasification, excess steam is necessary to promote the reaction but can reduce the thermal efficiency of the process [42]. The present of hydrogen can inhibit the reaction rate, an effective way is to remove hydrogen continuously [24]. Moreover, if hydrogen is sufficient, at the condition of high pressure and low temperature, char can be converted into methane assisted by catalysts [42].

Water-gas shift (WGS) reaction is also a major reaction in steam gasification, where all syngas compositions involve. This reaction promotes the hydrogen content in the syngas by decreasing CO. Above 1000°C, the reaction can achieve equilibrium state fast. The reaction rate depends on the temperature without catalysts, but it is not so sensitive to pressure. [24].

Table 2.7: Main gasification reactions [40]

No.	Reaction type	Reaction	Reaction heat ΔH^0 kJ/mol
		Char combustion	
R6	Partial combustion	$C + (1/2)O_2 \longrightarrow CO$	-111
R7	Complete combustion	$C + O_2 \longrightarrow CO_2$	-394
		Char gasification	
R8	Steam gasification	$C + H_2O \rightleftharpoons H_2 + CO$	+131
R9	Boundouard reaction	$C + CO_2 \rightleftharpoons 2CO$	+173
R10	Hydrogasification reaction	$C + 2H_2 \longrightarrow CH_4$	-75
		Homogeneous volatile reactions	
R11	CO oxidation	$CO + (1/2)O_2 \longrightarrow CO_2$	-283
R12	H_2 Oxidation	$H_2 + (1/2)O_2 \longrightarrow H_2O$	-242
R13	CH_4 Oxidation	$CH_4 + 2O_2 \longrightarrow 2H_2O + CO_2$	-802
R14	WGS reaction	$CO + H_2O \rightleftharpoons H_2 + CO_2$	-41
R15	Methanation	$CO + H_2 \rightleftharpoons H_2O + CH_4$	-206

2.5 Bubbling fluidized bed reactors

The reactors that have been conducted in plastic pyrolysis and gasification including fixed beds, fluidized beds, spouted beds, plasma reactors, where fluidized bed gasifier is the most popular for each type of plastic. Most of research related to PET pyrolysis and gasification was carried out in the bubbling fluidized bed (BFB), which is also the gasifier used in this project work [36, 48–51]. Therefore, in this section, knowledge of bubbling fluidization will be introduced, followed by recent research of bubbling

fluidized bed with PET pyrolysis and gasification.

2.5.1 Bubbling fluidization

Fluidization is defined as the operation through which fine solids are transformed into a fluid-like state through contact with a gas or liquid [43]. In the fluidized bed, the drag force of gas or liquid is offset particles gravity. Therefore, the particles are semi-suspended in the reactor [43]. Well-mixing and temperature uniformity are two essential characteristics of the fluidized bed. These features enhance the heat and mass transfer between solid and fluidized medium, so the reaction efficiency can be improved.

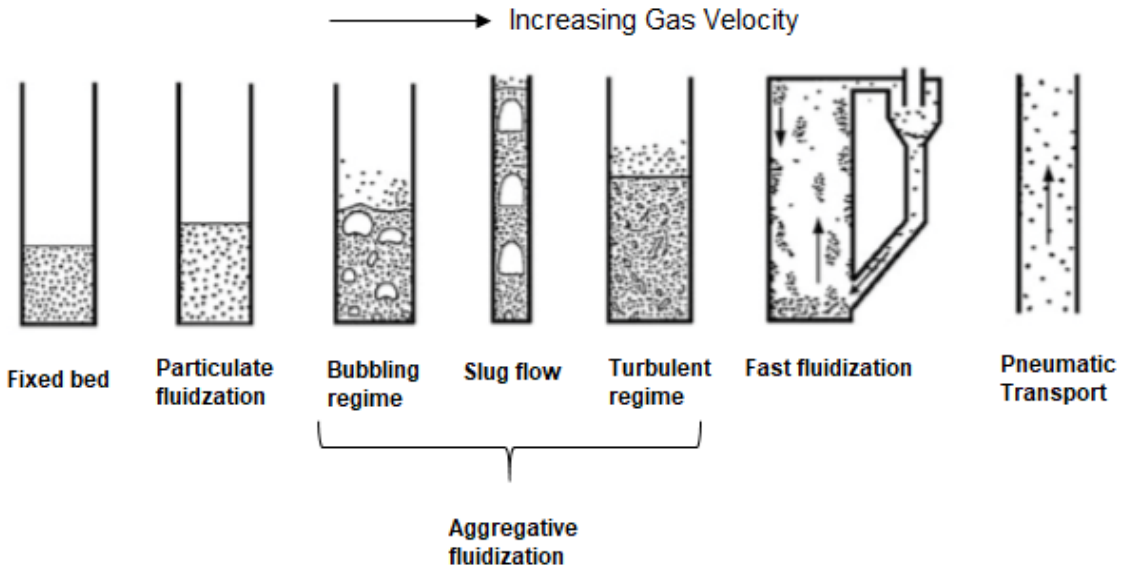

Figure 2.6: Scheme of fluidization regimes [44]

Fluidized regimes are determined by various fluidized medium velocities, as Figure 2.6 depicted [44]. A fixed bed refers to a bed of stationary particles when gas flow is low. With the velocity of gas increasing, the particles start to move. The critical value is known as the minimum fluidization velocity U_{mf}. For large and dense particles (Group B and D, the categories of particle groups based on density and particle size is shown in Figure A.1) bubbles will form when velocity exceeds U_{mf}, while the minimum bubbling velocity U_{mb} should be reached for smaller particles (Group A). Increasing fluid flow velocity causes larger and larger bubble size until the velocity of U_c at which large size bubbles tend to break and transfer into the turbulent regime. Thus, for bubbling fluidization regime, the superfacial velocity U is in the range of $U_{mb}<U<U_c$ [43, 45].

The minimum fluidization velocity is an important parameter for analyzing and design-

ing the fluidized bed. Other parameters such as the diameter of bubble are determined by it, even for group B and D, U_{mb}=U_{mf}. In the case of Re_p<10,

$$Re_p = \frac{\rho_g d_p U}{\mu} \tag{2.1}$$

the minimum fluidization velocity U_{mf} can be calculated by equation 2.2

$$U_{mf} = \frac{(\psi d_p)^2}{150\mu}[g(\rho_c - \rho_g)]\frac{\epsilon_{mf}^3}{1-\epsilon_{mf}} \tag{2.2}$$

where,
d_p : average diameter of particles, m; μ: dynamic viscosity of gas, Pa/s ;
ψ : sphericity of particles; ρ_c : density of particles kg/m^3 ; ρ_g : density of gas, kg/m^3 ;
ϵ_{mf} : the corresponding porosity of the bed at the state of minimum fluidization

For B and D particles, only the emulsion phase without bubbles can be observed when gas velocity is U_{mf}. The bed can be extended by feeding more gas. The open region above the bed is called freeboard, where the bubbles entrain some particles in their wake. The bubbles entraining particles can move upward employing momentum and local gas drag. Some particles will disengage from the bubbles due to the gravity force and return to the dense bed. This process can reduce upward particles flux in exponential order. After a specified height, the disengaged particles can be neglected, known as transport disengaging height (TDH). Only the particles whose terminal velocity is lower than the gas flow velocity can be pushed beyond TDH. TDH is another essential parameter for fluidized bed design. The profile of bubbling fluidized bed along the bed height is illustrated in Figure 2.7 [43].

Considering gasifiers, large fractions of volatiles can be released in the free board. Therefore, over-bed feeding is commonly used. Researchers suggested that endogenous bubbles may form around devolatilizing particles. The bubbles move up and the char particles fall down to the dense bed before reaching the top of TDH. Char gasification reaction can take place in dense phase or at the bottom of the free board while tar reduction occurs at the top of the freeboard, as Figure 2.8 shows [45, 46].

Particle agglomeration can be a serious problem for fluidized bed reactors. In the case of PET, bed material can adhere to the surface of sticky char residues, and the agglomeration will continue to grow, causing operating difficulties and bed defluidization. Arena & Mastellone investigated the defluidization phenomena during the pyrolysis of PE and PET in the bubbling fluidized bed. For recycled PET pyrolysis, the increasing of the ratio between the bed hold-up and PET feeding flow rate (W_{bed}/Q_{PET}) extended the

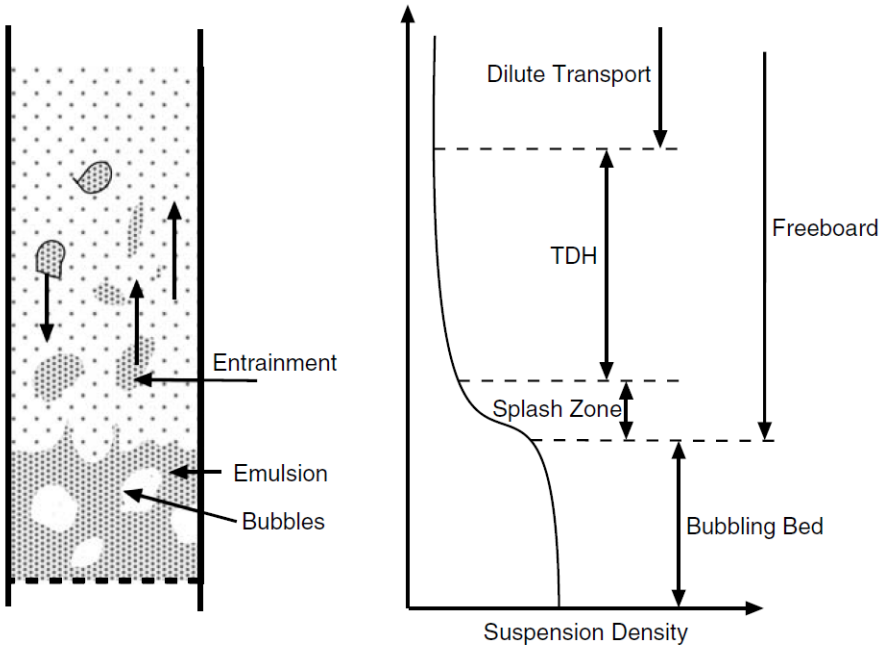

Figure 2.7: The profile of bubbling fluidized bed along the bed height [43]

defluidization time, and the same result was gained by rising bed temperature, while the gas velocity and bed material size had no effects. The authors proposed W_{bed}/Q_{PET}, which was key parameter for defluidization time and an operation criterion to avoid this phenomenon, providing an essential reference for fluidization optimization, W_{bed}/Q_{PET} = $62.8t^*$ (where t^* is the 2/3 of the critical time for defludization) [47].

2.5.2 PET pyrolysis and gasification in bubbling fluidized bed

PET pyrolysis in bubbling fluidized bed has been conducted by several researchers, while the studies about PET gasification were most about co-gasification with coal, biomass or other plastics. However, these results are still helpful to this project. This section will introduce some studies related to PET pyrolysis and gasification in bubbling fluidized bed. Table 2.8 exhibits the results obtained in different PET pyrolysis and gasification research carried out in bubbling fluidized bed.

Brems et al. [48] studied the kinetics and thermodynamics of PET pyrolysis reactions by using TGA and bubbling fluidized bed reactor. They injected batch PET (about 50g) in the reactor at the temperature of 450°C. The velocities of N_2 were $2U_{mf}$ and $5U_{mf}$ to test the influence of heating rate on the distribution of gas, liquid, and solid products due to their different heat transfer rate. The results are shown in Table 2.8.

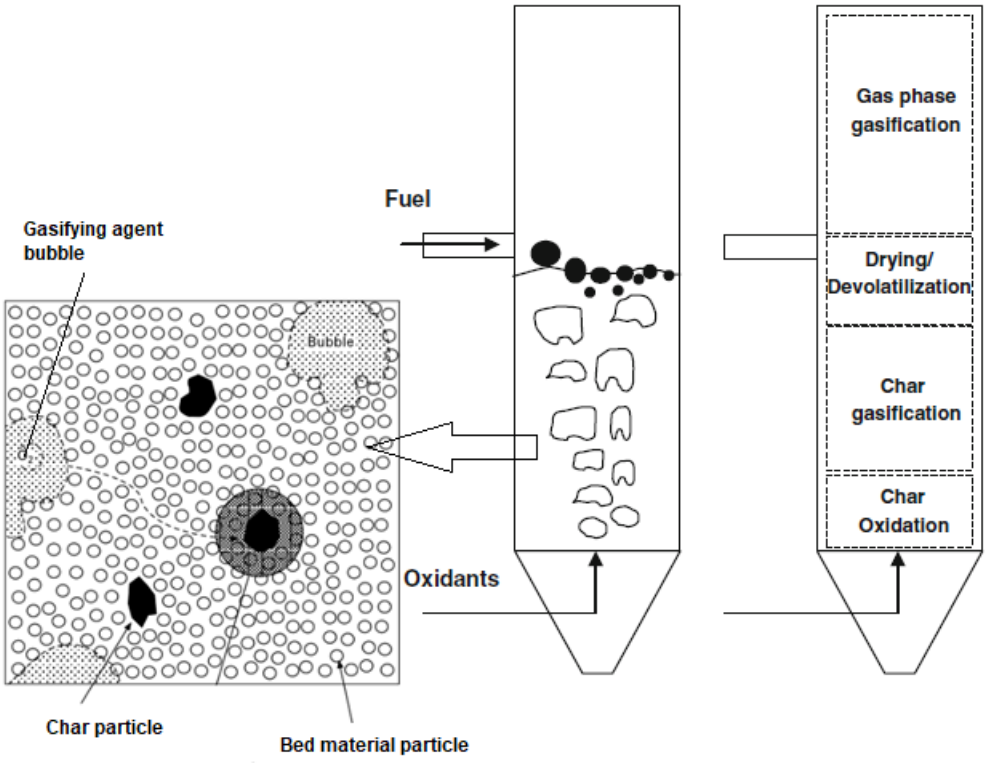

Figure 2.8: Generic bubbling fluidized-bed reactor schematization and process description. [45, 46]

Yoshioka et al. [36] studied the pyrolysis of virgin PET and recycled prepaid card PET. Two typed of prepaid card were selected as raw materials, containing 77% PET, 12% TiO_2, 5% Barium ferrite, 4% Netallic Ni, Fe, Mo (Material I) and 70% PET, 13 % TiO_2, 7% Fe_2O_3, 7% NiO (Material II) respectively. The virgin PET pyrolysis was carried out at the temperature of 510 and 630 °C and prepaid cards were tested at 630 and 730 °C with the bed material of quartz sand. They concluded that with the increasing temperature, acids disappeared even the presence of the metals can reduce acid formation significantly. For example, virgin PET pyrolysis at 630°C produced 16 wt% benzoic acid, while Material I generated 12% at 630°C and dropped to 0.22% at 730°C.

Robinson et al. [49] compared wood and wood-PET pellet gasification in air-blown bubbling fluidized bed. The wood-PET pellets were made at a mass ratio of 50:50, and the air flow velocity was 3.8-4.7 times U_{mf}. They observed that wood-PET pellets prevented coking above the bed compared to the mixture of wood and PET, so they thought there was intimate contact between the wood and PET in the wood-PET pellet. In addition, gases produced from wood-PET pellets tended to have a higher

Table 2.8: Results of PET pyrolysis and gasification in bubbling fluidized bed

Reference	[48]	[36]	[49]	[50]	[51]
Feedstock	PET (From soft drink bottles)	Virgin PET; Virgin PET + TiO_2	PET+ woodpellet (50:50)	PET+coal (23:77)	PET+olivehusk (25:75)
Bed material	Ballotini glass leads	Quartz sand	Olivine sand	Silica sand	γ-Al_2O_3;Ni/γ-Al_2O_3
Gasified agent	N_2	N_2	Air	10%(vol%) O_2 in N_2	steam+air
Fluidization velocity	2-5U_{mf}	-	3.8-4.7U_{mf}	-	33-67U_{mf}
Conditions	420-450°C	510-730°C	725-875°C ER:0.19-0.31	849-906°C ER:0.28-0.31	648-852°C ER:0.1 SF:0.4-1.08
Gas yield	16-18 (wt%)	31-40 (wt%)	-	-	-
Gas composition	-	H_2:0.09-0.79; CO:16-29; CO_2:13-25; CH_4:0.87-2.6 (wt%)	H_2:4.3-5.4; CO:8.9-12.7; CO_2:16.3-17.4; CH_4:2.6-3.0 (vol%)	H_2:11-18; CO:18-37; CO_2:17-7; CH_4:2-3 (vol%, 896°C, ER:0.28)	H_2:26.6-40.4; CO:9.0-27; CO_2:12.5-26.2; CH_4:5.5-8.9 (vol%)
Liquid yield	55-65($2U_{mf}$); 58-66($5U_{mf}$) (wt%)	2-12(wt%)	-	-	-
Solid yield	24($2U_{mf}$); 16($5U_{mf}$) (wt%)	8-49(wt%)	-	-	-
Tar	-	-	63-145g/m^3	7893mg/m^3	6.96-152.1g/m^3

concentration of CO, CO_2, $C2$ and $C3$ but lower hydrogen and methane, which leads to lower heating value than gas produced from the wood pellet. Tar formation was also remarkable in wood-PET pellet, secondary air was introduced into freeboard to reduce tars but could not meet the standard of engine application. This fact proves that plastic gasification can produce high content of tar.

Pohořelý et al [50] explored co-gasification of 23% PET and 77% brown coal in a fluidized bed with the medium of 10 vol % O_2 in bulk of nitrogen. They chose 23% PET in the mixture because, in their previous experiment, PET composition higher

than 30 % enlarge the potential of particle agglomeration. The TGA results showed that PET was more reactive and had higher volatiles than coal. So, free oxygen can immediately react with PET and much higher bottom char formation than single coal gasification. As the similar result obtained before, tar content was more than three times higher in coal blending with PET than single coal. Growing bed temperature can increase the content of CO and hydrogen, whereas the freeboard temperature plays a less important role since char gasification mainly takes place in the bed.

Brachi et al [51] reported the co-gasification of the olive husk (75% wt) with PET (25% wt) pellets and the same proportion of olive and tyre pellets. They focused on the end use of syngas product for producing bio-methanol, where the mixture of steam and air was used as the gasifying agent so that high yield of CO and H_2 can be obtained. From the experiments, they discovered that feeding in the middle bed instead of splashing zone removed tar significantly, and the products of tar cracking were mainly light hydrocarbons. Besides, temperature and steam to fuel ratio (S/F) exerted the greatest effect on gas product composition: higher temperature and S/F ratios can increase higher content of hydrogen and CO_2 but decreased CO and methane.

2.5.3 Dual fluidized bed

Dual fluidized bed (DFB) gasifiers have been applied to industrial scale successfully in Austria, Germany, and Sweden. The basic principle of DFB is shown in Figure2.9. Gasification and combustion take place in the interconnected bubbling fluidized bed and circulating fluidized bed respectively. Some ungasified char in bubbling fluidized bed is transported with bed materials into combustors. The combustion of char and additional fuels with air can provide heat for gasification. The bed material can be separated by the cyclone and return to the BFB [52–54].

Wilk & Hofbauer [54] investigated PE, PP, and mixtures of PE+PS, PE+PET and PE+PP in the DFB gasifier, in which the blending of PE+PET was 20%:80%. Steam was used as gasifying agent and olivine is the bed material. The results showed that the mixture of PE+PET produced more CO and CO_2 than others due to high oxygen content, accounting about 50% of gas products. Higher tar concentration was obtained from pure PP and PE gasification, but the lowest tar formation occurred in PE+PP. The reason might be PE and PP interacted with each other and promoted the reforming reactions. PE+PET produced a large amount of biphenyl that contains two benzene rings connected by a single C-C bond.

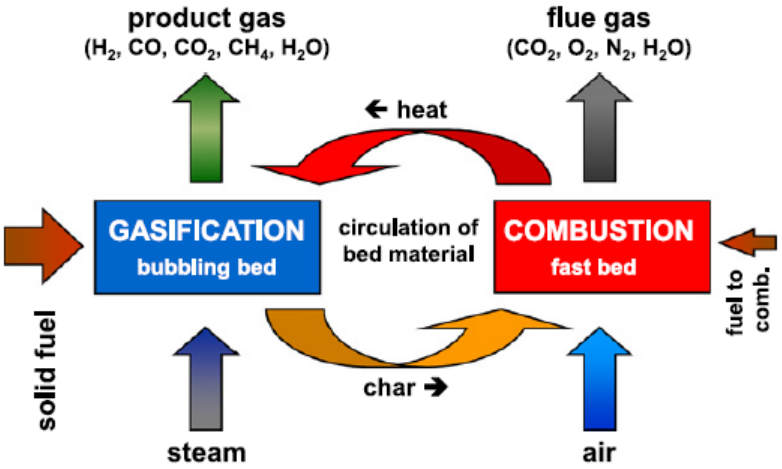

Figure 2.9: Basic principle of the dual fuel gasification technology [54]

2.6 Syngas applications

Syngas, mainly consisting of CO, H_2, CH_4, and CO_2, is the aim product of gasification and essential raw material for power generation and chemical industries. The feedstock, process, and operational conditions of syngas production determine the energy quantity and individual gas distribution. The application of syngas is illustrated in Figure 2.10 [55].

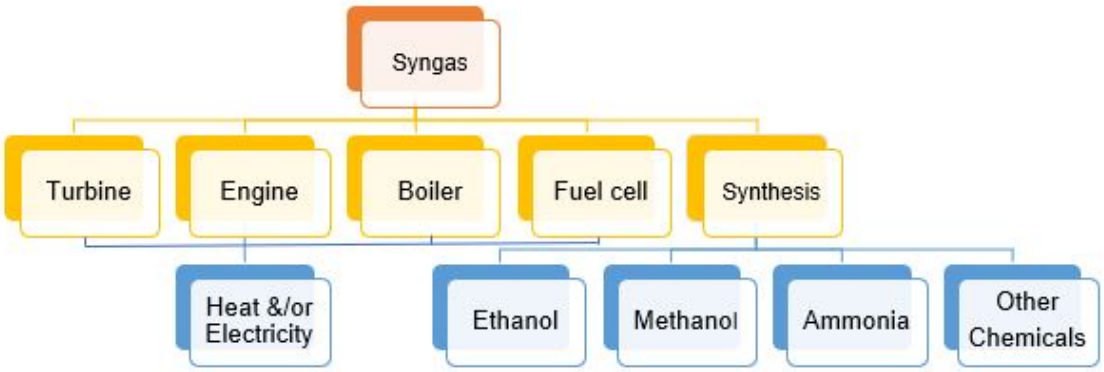

Figure 2.10: The applications of syngas [55]

2.6.1 Heat and power generation

Syngas can be directly used as combustible gas in the gas turbine, engine or boiler to produce heat and power. Quaak et al. reported that compared with combustion,

gasification can improve the electrical efficiency in power plant and CHP, but lower heat production in CHP and gasification process was economically competitive with combustion if it was in small scale [56]. In the gas turbine, in order to avoid the corrosion of blades, tar content in syngas should be less than 5 mg/Nm^3 [57]. Besides, since the internal combustion engine are mainly designed for gasoline and diesel, syngas can co-combust with liquid fuels without the modification of injection system [57]. Syngas can also be introduced into the anode of fuel cells to produce electricity, but the tar content is rigorous ($< 1\ mg/Nm^3$) because high tar composition can result in carbon deposition on the surface of anode [57, 58].

In Europe, several biomass gasification CHP plants have been constructed and operated successfully. A Danish CHP, Skive Fjernvarme plant is one of them with the load of 6 MW_{el} (3×2MW$_{el}$ internal combustion engines) and 11.5 MW_{th} (produced by 2×10MW$_{th}$ boilers) for district heating. A bubbling fluidized bed is used to gasify wood pellets, and the maximum capacity of fuel input is $28MW$. The gasifier is operated at 850 °C and maximum 2 bar over atmospheric pressure. Air works as the gasifying agent and the bed material is dolomite. The gas product consists of H_2: 16%, CO:20%, CO_2:12%, and CH_4:4% in vol% with a heating value of $5MJ/kg$ [59]. The gas product is cleaned by a tar reformer, a gas filter, and a gas scrubber [59, 60].

2.6.2 Fuel synthesis

The second application of syngas is producing fuels, including gas (H_2 and CH_4) and liquid (methanol, ethanol, dimethyl ether (DME), and Fischer-Tropsch diesel). Table 2.9 [61] illustrates the required H_2/CO ratio and corresponding operational conditions for different fuels production.

As Table 2.9 reveals, all of these reactions must be carried out at higher pressure and assisting by catalysts. For example, the syngas can be converted into methanol with the H_2/CO ratio of 2 (mol/mol) at the pressure of 50-100 bar.The temperature is 250 °C, at this relatively low temperature, the catalyst ZnO, Cu or Al_2O_3 has remarkable performance. The presence of CO_2 is necessary for raising the reaction rate by the factor of 100 [61].

Fischer-Tropsch Synthesis (FTS) is the process to synthesis fuels such as methane, ethane, ethylene, LPG (C3–C5), fuel (C5–C12), gasoline (C13–C22), and waxes (C23–C33) by H_2 and CO with zero carbon emissions. This process makes it possible to produce linear chains with avoiding sulphur and other impurities. The distribution of the products depend on the catalysts, residence time, temperature and the ratio of H_2/CO [61].

Most of the syngas for fuel synthesis applications are still in lab scale. The main challenge of industrial scale-up should be the high pressure, which is a risk for gasifier

Table 2.9: Conditions for syngas conversion [61]

Fuel	H_2/CO (mol/mol)	Temperature (°C)	Pressure (bar)	Catalysts	CO_2 (mol/mol)
Methanol	3	350-450	250-300	ZnO/Cr_2O_3	4-8% v/v
	2	200-300	50-100	$Cu/ZnO/Al_2O_3$	
Ethanol	2	230-300	55-65	Rh catalysts	<1-5 $mol\%$
	$\cong 1-1.2$		70-105	MoS_2	< 5 mol %
DME	$\cong 1$	methanol synthesis	methanol synthesis	γ-Al_2O_3, additives	H_2/CO_2=3
	$\cong 2;3$	200-300	30-70	CuO-ZnO-MnO and zeolite	$CO_2/(CO_2+CO)$ <0.2
FTS	0.6-1.7;2(K as promoter)	300-350	10-40	Fe catalyst	H_2/CO_2=1;3(K as promoter)
	2.0-2.15	200-240	7-12	Co catalyst	H_2/CO_2=3
Hydrogen	$\geqslant 2$	200-1100	1-30	Ni,Fe,Mo catalysts	-
Synthetic Natural Gas	$\geqslant 3$	200-450	1-25	Ni,Fe,Co,Rh catalysts	H_2/CO_2=4

with very high investment and operational cost. Additionally, the strict limitations for impurities inhibit the commercial application of syngas for fuel synthesis, as Table 2.10 shows.

Table 2.10: Syngas purity stardard for fuel synthesis process [61]

	Methanol(mg/m^3)	Ethanol($ppmv$)	FTS($ppmv$)	Hydrogen($ppmv$)	SNG($ppmv$)
PM	<0.02	0	0	0	0
Tars	<0.01	<0.5	<0.01	<1-2(mg/Nm^3)	<2-5(g/Nm^3)
Alkali	<0.005($ppmv$)	-	<0.01	-	-
Nitrogen	<0.1	<1-10	<0.02-10	1-10	<30
Sulpher	<1	<1-50	<0.01-1	<1-50	<0.1
Halides	<0.1	-	<0.01	-	<10

3

Experimental Facilities and Design

This chapter introduced the materials, the facilities, procedure and design of the experiments. The thesis aims to analyze the influence of operational conditions on PET steam gasification product distribution in the BFB. Therefore, in BFB gasification experiments, different agents such as air, steam and their mixture were tested by batch experiments. Steam was selected to investigate the effect of temperature, residence time as well as steam to fuel ratio for the continuous feeding. In addition, TGA was performed to gain a comprehensive understanding of the thermal degradation of PET under different heating rates as well as bed interation. Virgin PET is the feedstock in most experiments, and real PET as well as PE, were also used for comparison in TGA and batch experiments.

3.1 Materials

Most of TGA, pyrolysis, and gasification experiments were carried out with the fuel of virgin PET, others such as PE and real PET were also applied to compare with the results of virgin PET. Real PET was from plastic bottles, cutting into small pieces. The ultimate analysis of PET and PE have been done by several researchers; the values were almost similar. The range of results are listed in Table 3.1

Table 3.1: Ultimate analysis of PET and PE (wt% dry basis)

	C	H	O	Others	Reference
PET	62.0 - 63.0	4.06 - 5.2	32.69 - 33.69	0 - 0.11	[50, 62, 63, 75, 77]
PE	84.97 - 86.66	13.26 - 14.57	0 - 0.32	0 - 0.23	[54, 63, 75]

The primary function of bed material is the transfer of heat, but sometimes the bed material can be catalytically active [64]. In this project, olivine is used as fluidized bed material, because it has good mechanical properties and moderate activity for tar cracking [54]. Mastellone and Arena even reported that olivine was effective for tar removal in plastic waste gasification, but the carbon can deposit on the surface of the olivine particle to deactivate the function as catalysts [65]. Bauxite is compared with the performance of olivine by means of TGA. The composition of olivine and bauxite are shown in Table 3.2 [66].

Table 3.2: Compositions of olivine and bauxite (wt%) [66]

	SiO_2	Al_2O_3	Fe_2O_3	Ti_2O	MgO	Cr_2O_3	NiO
Olivine	41.7	0.46	7.4	-	49.6	0.31	0.32
Bauxite	6.5	88.5	1.1	3.0			

3.2 TGA

Thermogravimetric analysis (TGA) is a remarkable method to investigate the continuous mass loss of a substance by heating or cooling the sample at a constant temperature in a defined atmosphere. The results of TGA are described as a TG curve that mass loss is dependent on temperature or time. The curve shows the steps of volatile components loss, decomposition, black carbon reactions (gasification and combustion at different atmosphere) and residues. Therefore, the decomposition process can be obtained, which is valuable for further research. The first derivative of TGA respect to time is so-called DTG telling the rate of weight loss [67].

3.2.1 TGA701 and its operation

The TGA instrument used in this project is LECO TGA701 that consists of a computer and a sample furnace with 19 crucibles, as Figure 3.1 shows [68, 69].

Figure 3.1: TGA701

The operation of TGA701 is easy to follow. After the samples adding, the carrier gas is fed into the system to remove the air in the furnace. The samples are indexed to the balance position automatically. The percentage of weight loss is measured and

reported as curves on the computer. Some parameters of TGA701 are illustrated in Table 3.3 [69].

Table 3.3: Main parameters of TGA701

Sample Size	Maximum 5g	Balance resolution	0.0001g
Temperature range	100-1000°C	Maximum Ramp Rate	Ambient to 104°C 15°C/min
Gas Flow rate (l/min)	3.5 5.0 7.0 8.5 10.0		104-1000°C 50°C/min

3.2.2 TGA experiment design

The TGA experiments aim to answer following questions that can provide useful imformation for bubbling fluidized bed experiment:

1. How does PET thermal decomposition profile look like?
2. What are the difference between PET and PE TGA curves?
3. How much does moisture, volatiles, fix carbon and ash contain in virgin PET?
4. How does heating rate influence PET TGA curves?
5. Do virgin PET and real PET TGA curves differ?
6. Can distinct bed materials and their amount affect the decomposition?

Table 3.4: TGA experiment design

Crucibles No.	Samples composition	Abbreviation	Questions can be answered
(1),(7),(13)	1 g Virgin PET	VPET	1,3
(2),(8),(14)	1 g Real PET	RPET	5
(3),(9),(15)	1 g PE	PE	2
(4),(10),(16)	0.95g Virgin PET + 0.05 g Olivine	VPET+0.05O	6
(5),(11),(17)	0.9g Virgin PET + 0.1 g Olivine	VPET+0.1O	6
(6),(12),(18)	0.9g Virgin PET + 0.1 g Bauxite	VPET+0.1B	6

The minimum air or oxygen flow rate can induce combustion instead of gasification. Therefore, only N_2 pyrolysis was conducted. The mass of all samples is 1g, and the gas flow rate was kept as constant (Medium level, 7.0 l/min). First, the temperature was increased to 110 °C to release all moisture. After that, heating the sample up to 900 °C so that volatiles left entirely. To analyzed the amount of fix carbon in the char, the system was cooled down and N_2 will be switched to O_2 to the burn the remained char after the specific time. Samples adding can be designed as Table 3.4 shows to solve questions 1,2,3,5 and 6 at specified heat rate. In each experiment, 18 crucibles

are divided into the same 3 groups to repeat, and 6 in each group are with different samples were loaded together. Because the maximum temperature ramp of TGA701 is 50°C/min at the higher temperature, the PET N_2 pyrolysis TGA profiles with the heat rates of 10°C/min, 30°C/min and 50°C/min were investigated. Then, question 4 can be answered.

3.3 Fluidized bed pyrolysis and gasification experiment

3.3.1 Reactor system

The pyrolysis and gasification experiments were carried out in a lab scale 253 MA steel reactor whose dimension is with the height of 1.27 m and 77.9 mm inside diameter (see Figure 3.2). The fluidization gas (N_2, air or steam) was fed (and mixed if required) in the windbox and blew through the distributor with 61 holes (diameter: 0.8mm) to the bubbling fluidized bed. The distributor was designed to provide a good gas distribution in the bed by the suitable pressure drop, meaning that the quality of fluidization and the amount of bypassing gas can be influenced by the distributors [70]. A ring above the distributor was used to mix the tracing gas with the fluidized gas evenly.

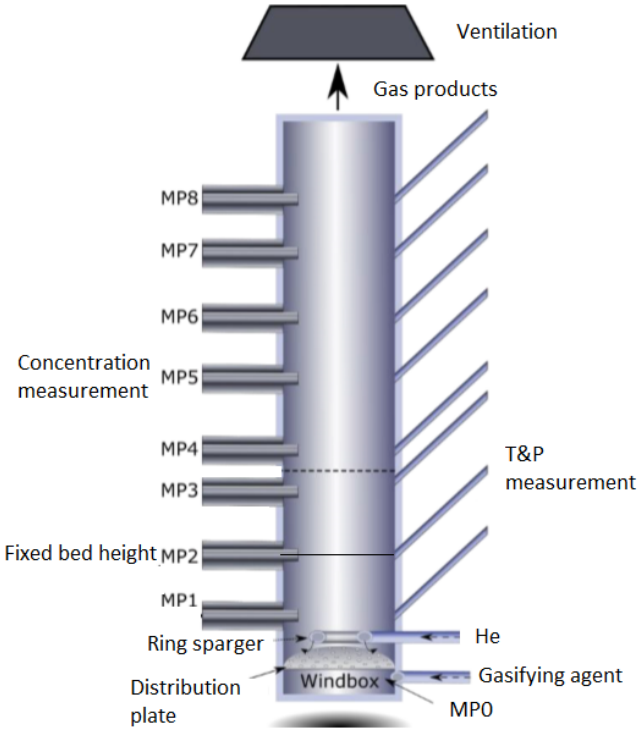

Figure 3.2: Schematic of the BFB reactor system [71]

Along the reactor, 8 vertical measurement points were for sampling or detecting prod-

ucts concentration and, the angled tubes at the same height opposite to vertical measurement points are used to measure temperature (by thermocouples) and pressure. The position of measurement points are illustrated in Table 3.5. The feeding system was installed at the top of the reactor that was heated by an electrical furnace.

Table 3.5: The position of measurement points [71]

Position	MP1	MP2	MP3	MP4	MP5	MP6	MP7	MP8
Distance above the distribution plate (cm)	3.65	8.88	13.65	15.65	31.65	47.65	73.65	79.65

3.3.2 Bed material

Olivine is used as bed material, and the minimum fluidization velocity U_{mf} in different gasifying agents were calculated by Equation 2.2, see the results in Table 3.6. Since olivine is Group B particles, bubbles can appear when the velocity is higher than U_{mf}.The range of bubbling fluidization gas velocity conducted by some researchers varied from 2 to 6 times the U_{mf} [48, 49, 66]. Considering the restriction of maximum gas flow rate that can provide is 10 l/min (at 20 °C), the gas feeding velocity is in the range of 2 - 3 U_{mf}.

Table 3.6: Physical properties and minimum fluidization velocities of olivine

Particle dencity ρ_c (kg/m^3)	Average particle diameter (μm)	U_{mf} (m/s at 750°C)		
		N_2	Air	steam
3300	288	0.043	0.042	0.048

3.3.3 Feeding system

The feeding system consists of a vibrating dosing system. It can be regulated either by the voltage input, with increasing voltages increasing speed, or by changing the operation mode, as Figure 3.3 shows.The feeding rate of PET was set as 0.8 g/min by setting the voltage of 105 V. The weight was measured at the start and end of the experiment, as the feeding rate is not necessarily accurate. The weight difference and time instead will be more precise as an average of the feeding rate.

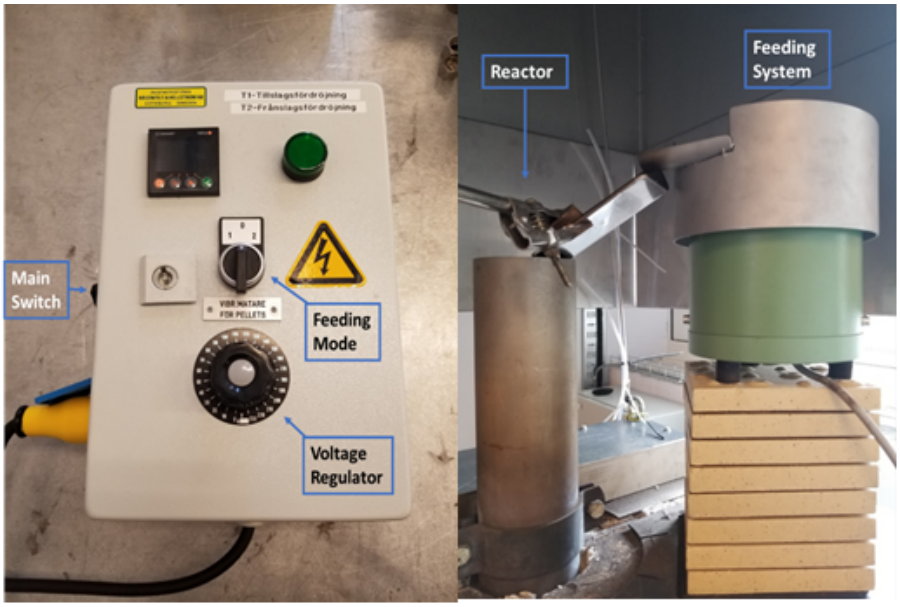

Figure 3.3: Main cabinet (left) and the feeding system on the reactor (right)

3.3.4 Experimental conditions

PET can be decomposed in the atmosphere of N_2, air (or O_2) and steam as well as their blendings, but in this project, steam was selected as the main gasifying agent, and N_2 pyrolysis and air gasification was compared with steam gasification. As described above, PET air gasification would generate high content of CO and CO_2, which constrained the application of syngas products. Furthermore, syngas product can be widely applied to energy and fuel production if hydrogen content is enhanced by using steam as a gasifying agent. PE and real PET were also investigated to compare with virgin PET pyrolysis and gasification. Batch feeding of 2g VPET, PE and 1g RPET were carried out in these trials.

Temperature is a key parameter for steam gasification. Therefore the influence of temperature on PET gasification should be investigated. Even though high temperature (>1000°C) gasification has been proposed recently, the maximum temperature that the furnace can heat up is 1000°C. Together with the TGA results showed at higher heating rates, reaction temperature should be higher than 600°C to guarantee the completed devolatilization process. Therefore, the range of temperature will be studied is 700 - 800 °C. The second reason is based on Figure 2.5, a higher temperature can induce the formation of secondary and tertiary tars whose cracking involves a great challenge. In this range of temperature, secondary and tertiary tars can be minimized or even avoided.

The temperature was specified at 750 °C for other experiments since PET, PE pyrolysis and gasification reactions completed or nearly completed. All feedstock feeding

flow rate was controlled around 0.8 g/min due to the limitation of the reactor size. If feeding is too fast, PET can be burnt at the inlet of the feeding where oxygen is sufficient for combustion, and even flame can be seen. The amount of steam also determines the hydrogen yield, therefore, the steam/fuel (S/F) ratio will be investigated. The accuracy of steam generator machine determines 1 - 3 g/min (S/F ratio: 1.25 - 3.75) is reliable. However, this range of steam flow rate is not sufficient for particles fluidization, therefore, N_2 can assist steam to fluidized bed material particles. Residence time is another essential operational parameter which can be determined by gas flow rate, setting 3.23 s - 4.83 s. The experiment conditions in all batch and continuous feeding are listed in Table 3.7.

Table 3.7: Bubbling fluidized bed experiment conditions

NO.	Feedstock	Reaction agent	Feeding Method	Temperature	Mass/flow rate	Variables
1	VPET	N_2	Batch	750°C	2g	-
2	RPET	N_2	Batch	750°C	1g	-
3	PE	N_2	Batch	750°C	2g	-
4	VPET	Air	Batch	750°C	2g	-
5	VPET	Steam	Batch	750°C	2g	-
6	RPET	Steam	Batch	750°C	1g	-
7	PE	Steam	Batch	750°C	2g	-
8	VPET	Steam + air	Batch	750°C	2g	-
9	VPET	Steam	Continous	-	0.8g/min	Temperature 700-800°C
10	VPET	Steam	Continous	750 °C	0.8g/min	Residence time 3,2 - 4,8s
11	VPET	Steam	Continous	750 °C	0.8g/min	S/F Ratio 1.25 - 3.75

Because the position of the measurement point is at MP5, the residence time can be computed to make sure gas velocity satisfies the range of bubbling fluidization. The residence time can be calculated by the following: As it is known, residence time (τ) is computed as Equation 3.1:

$$\tau = \frac{H_{MP5}}{100U} \tag{3.1}$$

where H_{MP5} is the height of measurement point MP5, cm.

The experiment design started from PET nitrogen pyrolysis at 550 °C and setting

the flow rate of N_2 feeding at 20 °C at the maximum value 10 l/min. Therefore, the superficial velocity in the reactor is calculated by Equation 3.2:

$$U = \frac{10 l/min \cdot \rho_{N_2,20°C}}{1000 \cdot 60 \cdot \rho_{N_2,550°C} \cdot A} \tag{3.2}$$

Since the volume flow rate will change with the temperature due to the different gas densities, the fluidized gas flow rate setting on the screen should be varied to guarantee the same gas velocity in the reactor. The volumetric flow rate set at 20 °C can be obtained by Equation 3.3:

$$\dot{V}_{20°C} = \frac{UA\rho_{g,at\,required\,temperature} \cdot 1000 \cdot 60}{\rho_{g,20°C}} \tag{3.3}$$

In this experiment, the required temperature is 750 °C, and fluidization gas is air or nitrogen. In steam gasification, 1 - 3 g/min cannot satisfy the same superficial velocity as before, therefore, additional nitrogen is necessary. The steam is generated by the machine at 190°C, the amount of required N_2 is computed as Equation 3.4.

$$\dot{V}_{20°C} = \frac{(UA - \dot{m}_{steam,190°C}/\rho_{steam,190°C}) \cdot \rho_{N_2,at\,required\,temperature} \cdot 1000 \cdot 60}{\rho_{N_2,20°C}} \tag{3.4}$$

Table 3.8: Parameter settings of N_2, air (at 20 °C) and steam (at 190°C) at different conditions

Experiment No.	Feedstock	Temperature	N_2	Air	Steam
1,2,3	VPET,RPET,PE	750 °C	8.04 l/min	-	-
4	VPET	750 °C	-	7.32l/min	-
5,6,7	VPET,RPET,PE	750 °C	6.69 l/min	-	2g/min
8	VPET	750 °C	6,45 l/min	0,84 l/min	2g/min
9-1	VPET	700 °C	7.09 l/min	-	2g/min
9-2,10-1,11-2	VPET	750 °C	6.69 l/min	-	2g/min
9-3	VPET	800 °C	6.30 l/min	-	2g/min
10-2	VPET	750 °C	5.10 l/min	-	2g/min
10-3	VPET	750 °C	4.03 l/min	-	2g/min
11-1	VPET	750 °C	7.36 l/min	-	1g/min
11-3	VPET	750 °C	6.02 l/min	-	3g/min

In the batch experiment, the steam air mixture as gasifying agent was used, the calculation of how much N_2 should be introduced is similar to this case. The amount of air used in this batch trial is 0.84 l/min, determined by the mass flow ratio between steam and air is 2. Besides, in the trials of the residence time change, the superficial velocity

cannot be kept as others, since residence time is known, the setting N_2 at 20 °C can be calculated by Equations 3.1 and 3.4. Parameter settings of N_2, air (at 20 °C) and steam (at 190°C) are shown in Table 3.8.

3.3.5 Product sampling and measurements

The products distribution indicates the quality of pyrolysis and gasification, so product measurement method is essential for the analysis. The raw product gas contains numerous components, ranging from inorganic gases to organic compounds, which can be divided into two groups: (1) μ-GC and (2) Tars and measured by different methods, which can be seen in Figure 3.4.

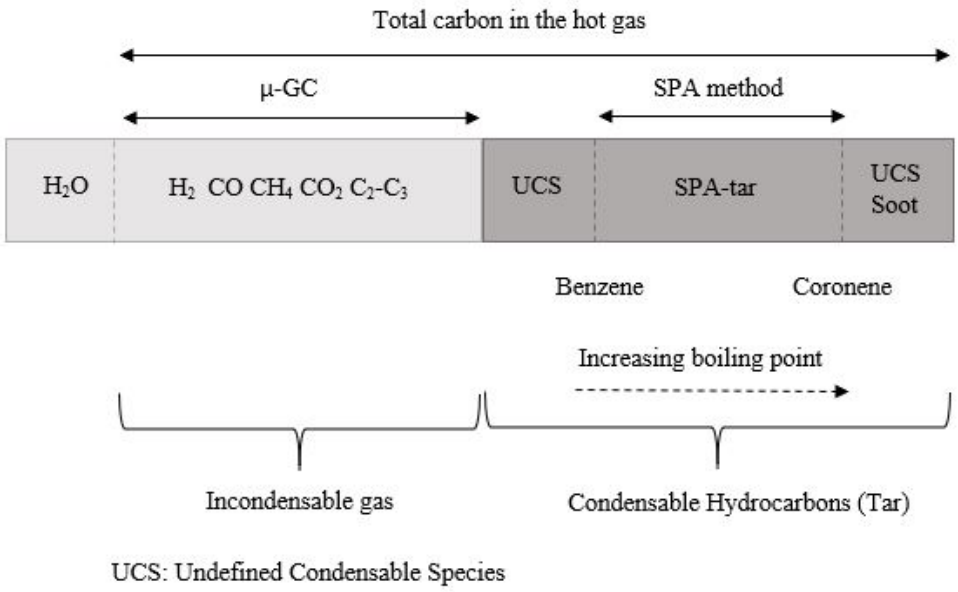

Figure 3.4: Products and measurement methods [66]

Helium tracing A small flow of high purity helium (0.05 l/min) is used as a tracer gas to quantify the total dry gas flow per unit of fuel and calculate the gas product distribution. Helium is introduced into the fluidized bed with the fluidization gas, all gas feeding is controlled by the flow rate controller.

Experiment procedure According the bed performance from previous experiments, MP5 (31.65cm) is a better option for collecting samples. Because the pressure was stable above MP4, where the region is free board zone . Also, MP7 and MP8 are very close to the outlet of the reactor where the temperature is much lower than the setting temperature. Gasbag and syringe were used to collect gas products and tars, respectively. The needle of the syringe was plugged into MP5. Once the fuel was fed into the reactor in the batch experiment, with the help of a pump, the raw gas products can pass through

the syringe where tars can be retained in the filter and be captured in the sample gas-bag. For continuous feeding experiments, sampling started 5 minutes after start feeding because the feeding system does not work stable during first several minutes. After 2 minutes of sampling, the gas bag and syringe should be sealed and removed. Choosing 2 min as sampling time because devolatilization and char gasification finished in 2 min in previous experiments. Moreover, for batch experiments, before each trial, the air should be introduced into the reactor as fluidization medium to burn the unreacted char entirely and eject the gas product to avoid disturbing the next trial. Then, the pump should be cleaned by pure N_2, and the cleaning gas returns to the fluidized bed.

Micro gas chromatography The cold gas product distribution was analyzed by micro gas chromatography (μ-GC).The μ-GC has two channels with He and Ar as the carrier gas. The equipment takes the sample to detect every 3 minutes. Before each testing, air will be introduced to clean the columns. The gases can be detected in this device are: CO, H_2, CH_4, CO_2, C_2H_6,C_2H_4,C_2H_2,C_3H_x and N_2 [66].

SPA method Tar collection were conducted by Solid-phase adsorption (SPA) method, where the tar is absorbed onto a solid-phase extraction column with an amino phase and then desorbed by a solvent [73]. In this case, Superclean ENVI-Carb/NH2 SPE columns were used in the syringes, with higher efficiency of BTX adsorption [66]. Tar sampling temperature should be kept around 350 °C to make sure all the tars are in the gas phase and not condensing before absorbed by the column. Subsequently, the sample columns should be stored at the temperature of -20°C in the fridge to avoid inter reactions of different tars. Tars were analyzed by GC equipped with a flame ionization detector(FID) and 28 tar species can be detected. These 28 tar species can be classified into 8 groups, which is illustrated in Table 3.9.

Table 3.9: Tar substance groups

Group	Tar substances
Benzene	Benzene
1-ring	Toluene, o/p-xylene, styrene, methyl-styrene
Biphenyl	Biphenyl
2-rings	Naphthalene,indene, 1,2-dihydronaphthalene, 1-methylnaphthalene, 2-methylnaphthalene
$\geq$ 3-rings	Acenaphthylene, acenaphthene, fluorene, phenanthrene, anthracene, xanthene, fluoranthenen, pyrene, chrysene
Phenols	Phenol, o/p-cresol, 1-naphtol, 2-naphtol
Furans	Benzofuran, dibenzofuran
Unknows	Species that can be found in the chromatograms but cannot be defined

4

Results and Discussions

4.1 TGA experiments

The TGA experiment results of the comparison of different plastics, heating rates and bed materials will be shown in this section to answer the research questions mentioned in 3.2.2. These results can provide important imformation for BFB experiment result analysis.

4.1.1 VPET, RPET and PE TGA profiles

Figure B.1 depicts TGA and DTG profiles of VPET, RPET, and PE at the heating rate of 50°C/min. The first step is the evaporation of the water. The results show that moisture can be neglected (0.15%), which is the prominent feature of plastics.

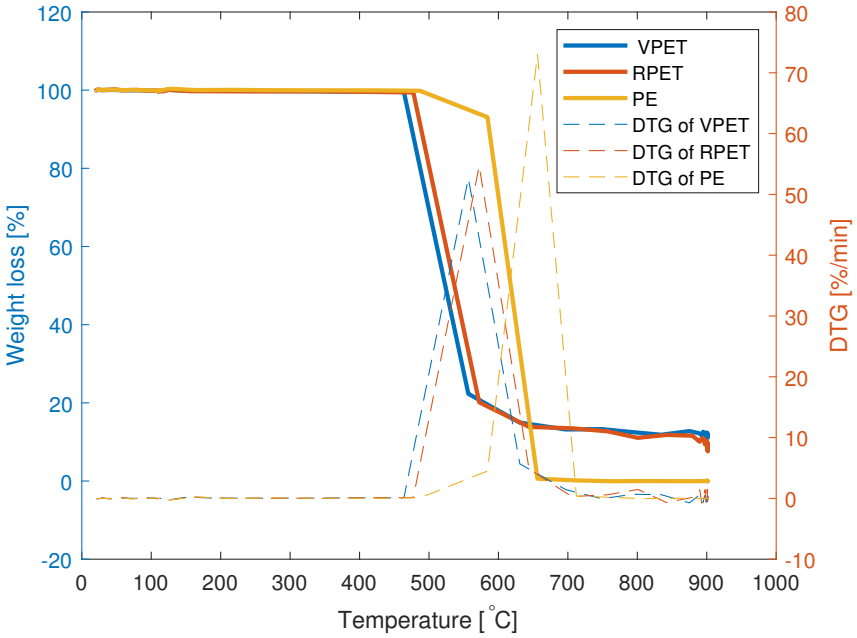

Figure 4.1: TGA of VPET, RPET and PE at 50°C/min

The majority mass loss is the process of devolatilization, sometimes referred to pyrolysis, and this process takes place very fast (80%/min), as the DTG curves illustrate, the

main weight loss of PET occurs at the temperature around 463 °C while PE is in the range of 487 °C. This information infers that the pyrolysis and gasification temperature must be higher than this range. Moreover, the volatiles component represents the most content in the plastic. In PET volatiles account for 88.39% whereas 99.96% of components in PE are volatiles. PET contains about 10 - 15 % fixed carbon indicating that char gasification can happen during the PET gasification process while PE cannot, answering Questions 1, 2 and 3 in 3.2.2. The comparison between TGA and DTG curves of VPET and RPET does not provide a remarkable distinction, but RPET contains a slightly more volatiles and moisture. Then, Question 5 has been solved.

All these results are similar to other PET TGA research. Meng et al.conducted the N_2 pyrolysis and CO_2 gasification of several types of plastics (PE, PS, PVC, and PET) on macro-TGA. It was observed that the residue of PE and PS were almost zero while PET remained the highest residues [74]. Despite different sources, TGA apparatus and heating rate, the significant mass loss of PET decomposition usually started in the range of 350-500°C [35,75–77]. Besides, Dimitrov et al. studied the TG curves of virgin PET, recycled PET, and contaminated PET flakes were nearly identical [82].

4.1.2 Influence of heating rate

The influence of heating value on VPET TGA is compared in Figure 4.2.The DTG results indicate that the heating rate could improve the main weight loss rate.

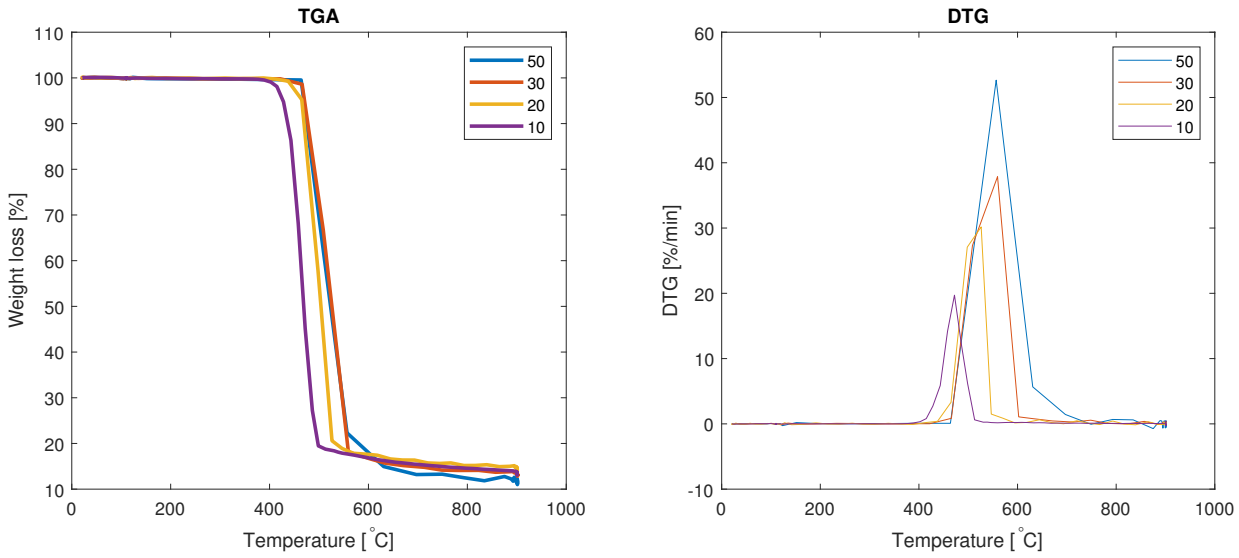

Figure 4.2: The influence of heating value on VPET TGA

In the original TGA experiment design, only three heating rates were planned to be investigated: 10, 30 and 50°C/min. After data analysis, it was observed that the devolatilization happens at the same time almost at the heating rates of 30 and 50°C/min.

Similar conclusion can be found in the two studies of PET TGA conducted by Brems et al [31, 48], the devotalization curves at very high heating rates are closed to each other in the period of main weight loss. This result indicates that in spite of particularly high heating rate in BFB, the devolatilization process would be similar to the heating rate of 50$°C/min$ in TGA. So in this section, the results of 50 $°C/min$ are discussed, other results can be seen in the Appendix B and C.

Therefore, the experiment of 20 $°C/min$ was added to investigate the influence of the heating rate between 10 and 30$°C/min$. Temperature range where decomposition occurred: the higher the heat range, the higher temperature that decomposition required if the heating rate of 10, 20, and 30 are considered. However, the effect of heating rate on the number of residues cannot be concluded, which was variable in different references. [48, 78–81]. The comparison of PET TGA between this project and other research is displayed in Table 4.1. Now the answer of Question 4 in 3.2.2 is clear.

Table 4.1: The comparison of PET TGA between this project and other research

Reference	Feedstock	Atmosphere	Heating value ($°C/min$)	Proximate analysis (wt%)				Main weight loss temperature range(°C)
				M	V	A	FC	
This project	VPET	N_2	10	0.07	86.81	0	13.12	389-499
This project	VPET	N_2	20	0.05	85.90	0.01	14.04	437-594
This project	VPET	N_2	30	0.11	86.90	0.01	12.99	465-602
This project	VPET	N_2	50	0.15	88.39	0.01	11.44	463-630
This project	RPET	N_2	50	0.26	91.46	0.01	8.26	477-644
This project	PE	N_2	50	0.03	99.96	0	0.01	487-656
This project	PE	N_2	10	0	100	0	0	462-550
[74]	PET	N_2	10	0.38	90.1	0.09	9.43	360-560
[74]	PE	N_2	10	0.17	99.8	0	0.02	440-560
[48]	PET	N_2	50	-	-	-	-	400-500
[48]	PET	N_2	120	-	-	-	-	400-490
[50]	PET	He	20	-	-	-	-	400-500
[78]	VPET	N_2	5	-	-	-	12.0	360-480
[78]	RPET	N_2	5	-	-	-	8.3	340-480
[80]	PET cloth	N_2	10	-	-	-	-	377-477
[80]	PET cloth	N_2	20	-	-	-	-	387-487
[81]	PET	N_2	10	0.4	85.7	8.3	6.0	380-470
[81]	PET	N_2	20	0.4	85.7	8.3	6.0	400-500

Note: M: moisture, A: ash, V: volatiles, FC: fixed carbon

4.1.3 The influence of bed material

Figure 4.3 illustrates the influence of bed material on PET pyrolysis at 50 $°C/min$. Bauxite can slightly bring forward the starting temperature of devolatilization process and slow down the weight loss rate.

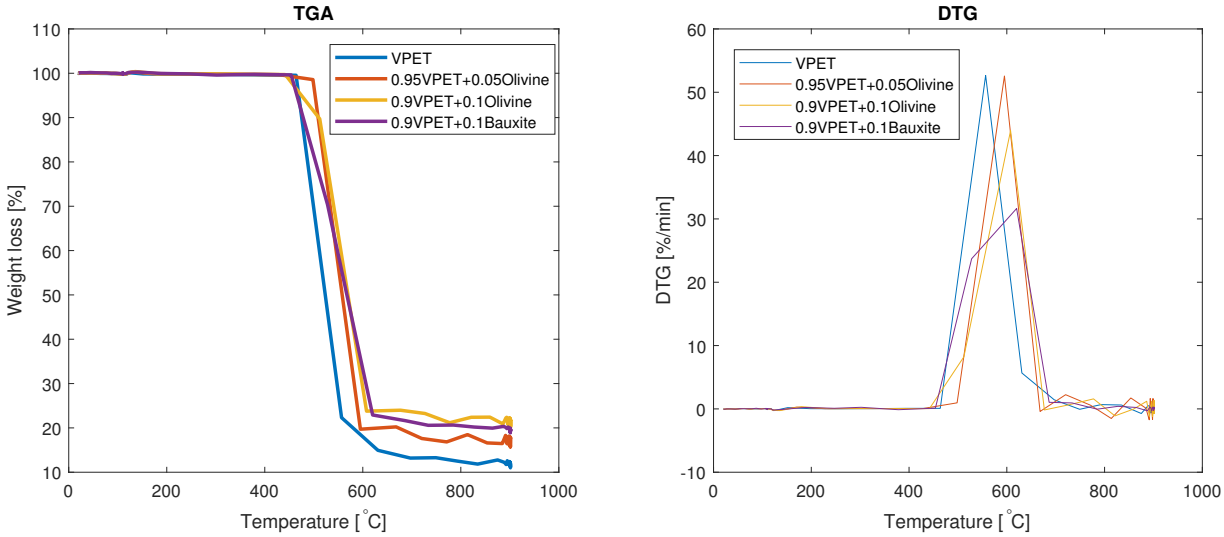

Figure 4.3: The influence of bed material on VPET pyrolysis at 50 $°C/min$ (wt%)

It is also observed that the ash content in all cases is less than that of the bed material added in the process. There are two possible reasons to explain this: the first one is olivine and bauxite containing some moisture, but this can be proved as a wrong guess by the data in Table 4.2. If there is some water in bauxite and olivine, it is not possible that the moisture content decreases compared with pure VPET. The same conclusion can be obtained by the results of olivine and bauxite TGA; no water is contained in the bed materials (see in Figure 4.4). The second one is bauxite and olivine involving the pyrolysis reactions. This should be proved by further experiments.

Table 4.2: Proximate analysis of PET with bed materials at 50$°C/min$ (wt%)

Feedstock	Moisture	Volatiles	Ash	Fixed carbon
VPET	0.15	88.39	0.01	11.44
0.95VPET+0.05Olivine	0.14	83.58	5.04	11.24
0.9VPET+0.1Olivine	0.13	78.82	9.84	11.22
0.9VPET+0.1Bauxite	0.09	80.69	9.29	9.93

Moreover, the influence of bed material on volatiles and fixed carbon can be evaluated

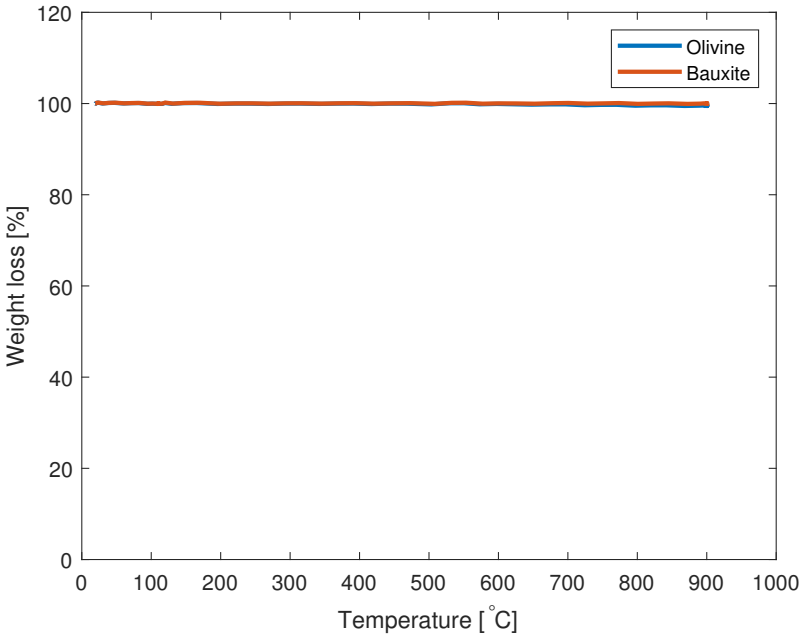

Figure 4.4: TGA of bauxite and olivine at $50°C/min$

by the factor of improvement δ that is calculated by Equation 4.2

$$\delta = \frac{wt\%_{VPET+bedmaterial} - wt\%_{pureVPET} \cdot f}{wt\%_{pureVPET} \cdot f} \tag{4.1}$$

where wt is the weight fraction from TGA proximate analysis result, f is the mass fraction of VPET. For example, the fixed carbon improvement factor of 5% olivine at 50 $°C/min$ can be computed by

$$\delta = \frac{11.24 - 11.44 \cdot 0.95}{11.44 \cdot 0.95} = 0.0348 \tag{4.2}$$

The δ values of volatiles show bed material has little effect on the volatile compositions, but as Figure 4.5 reveals, the amount of fixed carbon can be enhanced when the bed material appears. At all heating rates, 10% Olivine can improve the amount of fixed carbon by over 0.07. However, with the increased heating rates, 10% Bauxite cannot enhance the fixed carbon significantly, even at 50 $°C/min$, it can inhibit the FC formation. However, this conclusion can be applied to fixed bed experiment but not the fluidized bed in this project due to the distinct regimes of particle contact between bed material and fuels. The last question about bed material in 3.2.2 is solved.

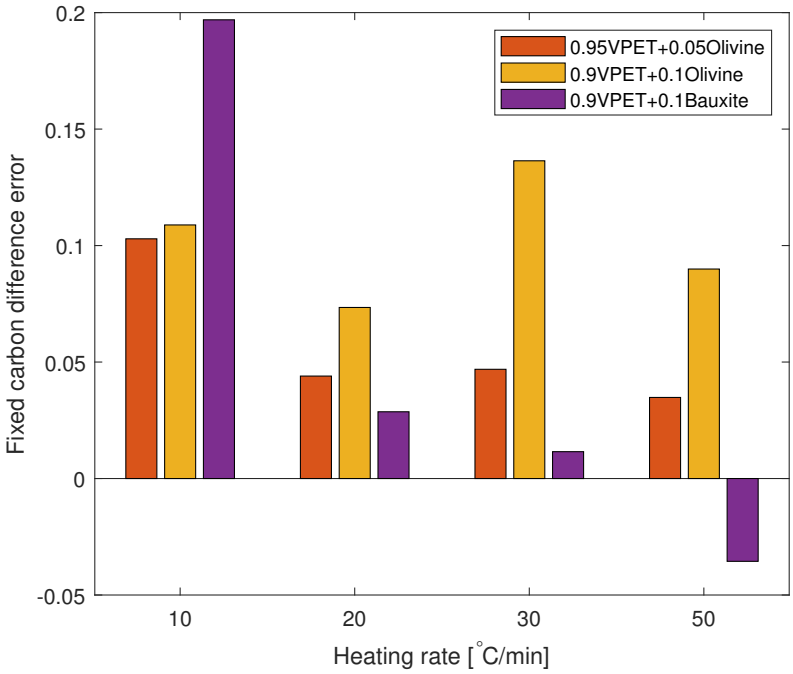

Figure 4.5: The influence of bed material on the fixed carbon improvement factor

So far, the questions proposed in 3.2.2 have been answered. These results can be applied to BFB experiment results analysis.

4.2 Batch experiment

The results of gas yield are expressed as mol/kg fuel for easing the data analysis for different applications. The original data was in $vol\%$, the conversion can be done by the Equation 4.3 with knowing the $vol\%$ of the tracing gas helium (Feeding rate :$0.05l/min$, Sampling time: $2min$).

$$n_i = \frac{0.05L/min \times 2min \cdot \alpha_i \rho_i \cdot 1000}{\alpha_{He} m_{feedstock} \bar{M}_i} \tag{4.3}$$

where, n is the molar gas yield, α is the volmetric percentage, ρ is the gas density (g/L), $m_{feedstock}$ is the mass of plastics and $\bar{M}$ is the molar mass (g/mol). The subscript i represents different components in the gas product.

The yields of tars are expressed in $g/kgfuel$ and mg/Nm^3 for different analysis. In results analysis and heating value calculation, g/kg will be used, which is computed as Equation 4.4.

$$m_j = \frac{m_{standard} \cdot Area\%_j}{1000 \cdot Area\%_{standard} m_{feedstock}} \tag{4.4}$$

where,m is the mass of each tar, j stands for various species of tars, $m_{standard}$ is the mass of standard solution for solving tars whose mass is 371.25 μg and $Area\%$ is the area percentage of each tar component read from GC results.

Table 2.10 gives tar concentration in the unit of mg/Nm^3. Equation 4.5 is useful.

$$m_k = \frac{\alpha_{He} m_{feedstock} m_j}{0.05L/min \times 2min \cdot 10^6} \tag{4.5}$$

The batch experiment aims to investigate the influence of different reaction agent and plastics on product distribution. Virgin PET is the main feedstock in this experiment. It is necessary to compare if the real PET decomposition product is distinct from virgin PET.

4.2.1 Virgin PET, Real PET and PE

Figure 4.6 shows the gas product of VPET, RPET, and PE pyrolysis. A remarkable characteristic of PET decomposition product is a high content of CO and CO_2 due to the oxygen in the molecules while PE pyrolysis produced a large amount of ethylene, the monomers of PE. But not only that, H_2 and CH_4 yields are much more than PET. Although VPET and RPET have similar TGA curves, the pyrolysis product distribution is different. It seems pyrolysis of RPET can produce much more gas, which coincides with the TGA result: in all cases, the volatile of RPET is higher than that of VPET.

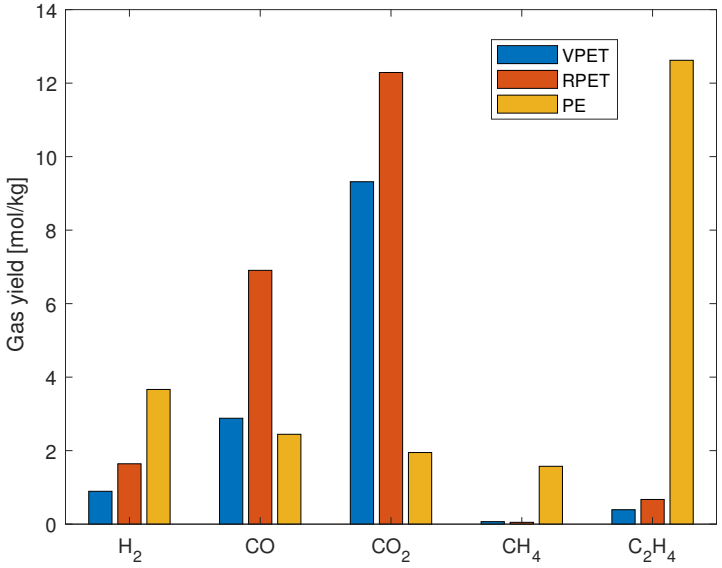

Figure 4.6: Gas product distribution of VPET, RPET and PE pyrolysis

Table 4.3 compares the results of this project with previous research. The results are quite different. Theoretically, CO and CO_2 cannot be generated during PE pyrolysis. Since some oxygen could remain in the bed, then part of gas products are partially or completely combusted. The higher temperature is helpful to release CO_2 according to 2.3. That is why CO_2 in this project is much higher than Yoshioka et al's.

Table 4.3: Results comparison of PET and PE pyrolysis (wt% of fuel)

Feedstock		Temperature	H_2	CO	CO_2	CH_4	C_2H_4	Other HC
VPET	This project	750 °C	0.18	8.07	40.99	0.31	1.10	-
	Yoshioka et al [36]	630 °C	0.13	18	17	1.9	-	1.33
PE	This project	750 °C	0.37	3.67	4.29	3.62	17.67	12.66
	Mastral et al [83]	730 °C	0.5	-	-	6.6	21.4	26.2

When it comes to steam gasification, as Figure 4.7 exhibits, all gas yields were improved. However, RPET steam gasification cannot produce as much hydrogen. At the atmosphere of steam, hydrogen production from PE gasification no longer has distinct advantages.

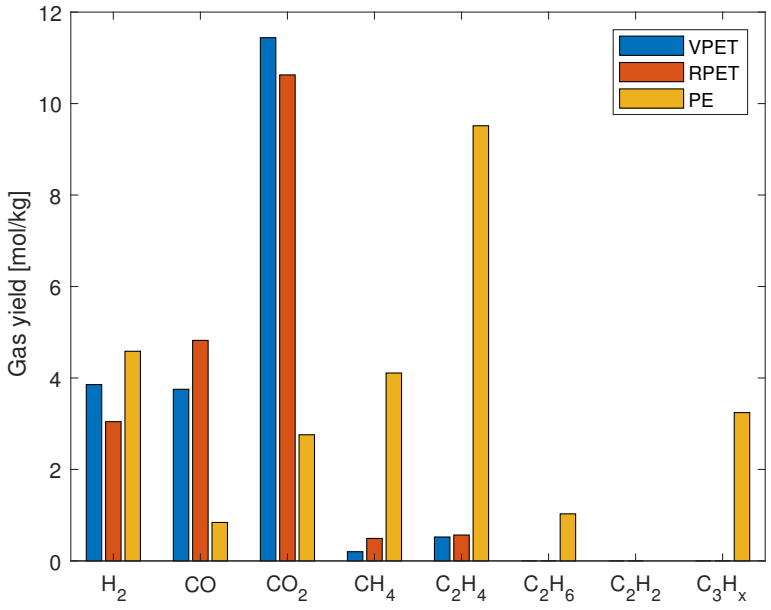

Figure 4.7: Gas product distribution of VPET, RPET and PE steam gasification

The tar formed by pyrolysis and gasification is compared in Figure 4.8. SPA can calibrate 28 species of tars, and other tars like benzoic acid are named as "Unknown".

In general, Benzene and other 1-ring aromatics are the dominant products. Virgin PET and PE steam gasification produced more tar than pyrolysis while real PET had the opposite result. Also, VPET produced more tars than RPET. No biphenyl can be found in PE decomposition products but other 2-rings aromatics were generated more by PE steam gasification. If compared pyrolysis with gasification, only RPET gasification has lower tars than pyrolysis. Because one of the repetitions result was missed, this result could be not so accurate.

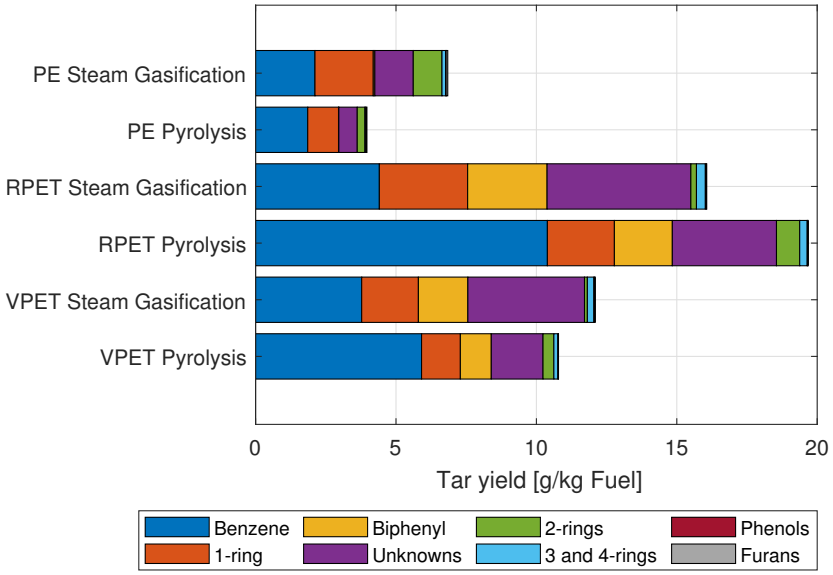

Figure 4.8: Tar distribution of VPET, RPET and PE pyrolysis and steam gasification

4.2.2 Gasifying agent

Three gasifying agents were reported in the literature: air, oxygen and steam. In this project, steam, air and their mixture were investigated to see their effect on the products, as Figure 4.9 displays.

Air gasification results in a very high concentration of CO_2 but steam cannot improve the hydrogen yield so significantly. Because the reaction rate of R6 ($C + (1/2)O_2 \longrightarrow CO$) is much faster than R8 (Char gasification $C + H_2O \rightleftharpoons H_2 + CO$) and other reactions. The concentration of each gas product of steam and air mixture gasification is between steam and air excluding CO. However, the results suggest that blending of air can prevent generating more H_2 and CO compared to pure steam gasification. Since PET contains oxygen in its molecule, oxygen and air are not the priority for its gasification. Compared pyrolysis and steam gasification, most CO and CO_2 in steam

gasification product was produced from pyrolysis process.

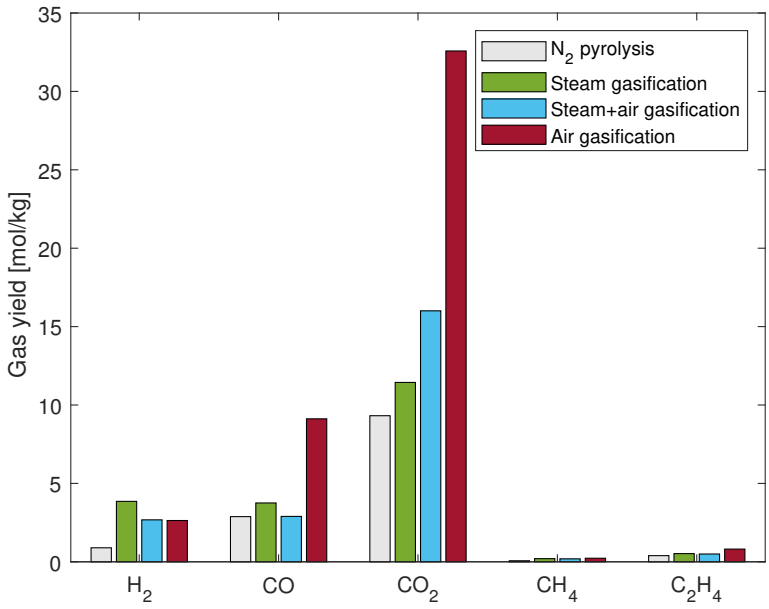

Figure 4.9: Gas product distribution of VPET at different atmosphere

Figure 4.10 shows the tar yield of VPET gasified at different atmosphere. The result indicates that PET gasified in the air can produce almost the same amount of tar as in steam. Therefore, the statement in Lopez, G et al 's review [1] that air can reduce tar formation cannot be applied to PET gasification. Air enhances the yield of Benzene, and in steam much more unknown tars can be calibrated. CO_2 produced in air gasification is not only from the reaction of carbon with oxygen in air but also from the loss of CO_2 in unknown aromatics.

4.2.3 Batch experiment bed performance

Figure 4.11 shows the temperature change at MP2 (the surface of the bed or splash zone) in the RPET steam gasification batch experiment at 750°C. The temperature of MP2 was investigated because the pressure and temperature of other MPs fluctuate slightly.At 843s to 851s, the temperature dropped from 756 °C to 753.4 °C indicating that Reaction R8 (endothermal reaction) occurred. Then, the temperature increased after reaction until the air was introduced into the system at 1035s. The air temperature was low so the temperature of MP2 decreased at first and the combustion of remaining FC and gas released heat so the temperature grew up to 759.5 °C. The declined temperature suggested all combustible substances were burnt out.

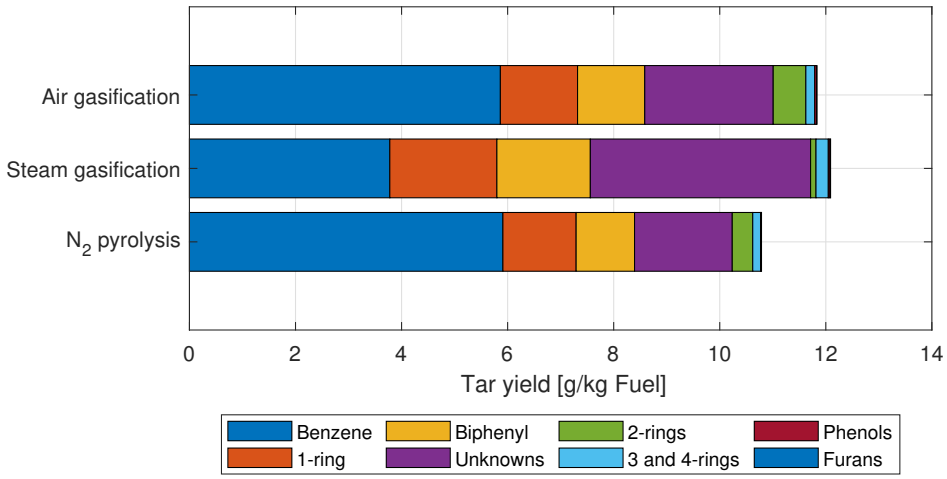

Figure 4.10: Tar product distribution of VPET at different atmosphere

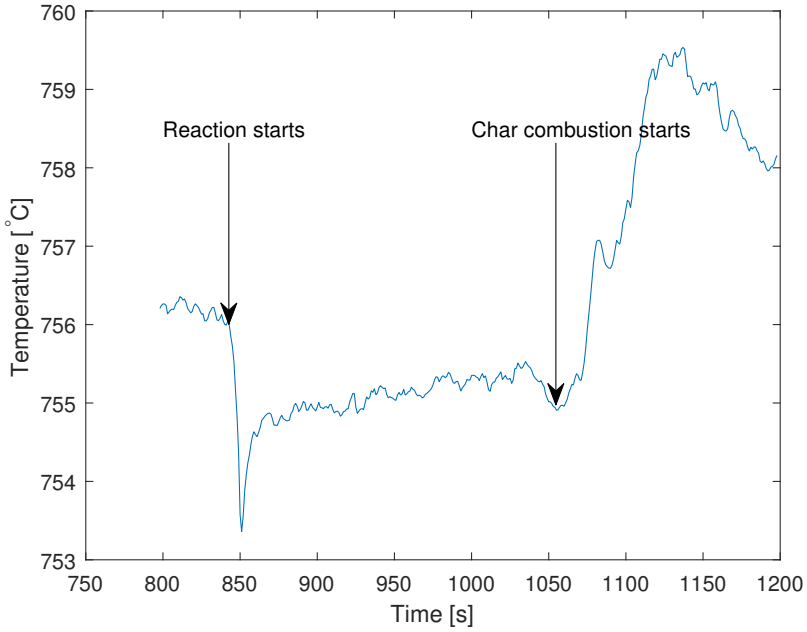

Figure 4.11: Temperature varies with time at MP2 in the BFB

4.3 Continuous experiment

Batch experiments can test the feasibility of an idea and investigate the details of the reaction. Nevertheless, continuous feeding is reliable to obtain some suggestions for industrial applications. The continuous feeding experiment is to examine how essential

operational conditions: temperature, SF ratio, and residence time affect the product distribution of PET steam gasification. The yields of gas and tar were calculated used the same equations 4.3, 4.4 and 4.5 in batch experiment.

4.3.1 Temperature

Figure 4.12 illustrates the gas production distribution changing with increasing temperature.The dash line represents the maximum CO_2 can be produced by PET pyrolysis, which is calculated by following: the monomer of PET ($C_{10}H_8O_4$, molecular weight: $192g/mol$) indicates that each monomer can release up to 2 CO_2 molecules. The molecular weight of PET is in the range of 30000-80000 g/mol [11], so the maximum CO_2 that 1 kg PET can produce by pyrolysis is:

$$\frac{1kg \times 10^3 g/kg}{30000g/mol} \times \frac{30000g/mol}{192g/mol} \times 2 = 10.24mol \tag{4.6}$$

All gas product yield rises due to the increasing temperature, but from 750 to 800 °C, the growth rate of H_2 is remarkable, whereas CO increases slightly. This can be explained by R2 ($CnHm + nH_2O \rightleftharpoons (m/_2 + n)H_2 + nCO$), which is an endothermic reaction. Therefore the rise of temperature is conducive to a shift of the reaction equilibrium towards the right side, which enhances the yield of H_2 and CO. Even though higher temperature motivates R14 ($CO + H_2O \rightleftharpoons H_2 + CO_2$) to move toward the left side, high S/F ratio in this case and the catalytic function of olivine affect the equilibrium more than temperature. Thus, H_2 has a faster growth rate than CO, and CO_2 yield exceeded the maximum CO_2 generated from pyrolysis process. Moreover, at 700 °C, char gasification reaction could not start, so that is why the H_2 and CO yields are much lower. High temperature results in the break of more C-C bond so at high temperature, the yield methane is more than that of $C_2 + C_3$.

The most likely PET pyrolysis reaction illustrated in Figure 2.3 indicates with higher temperature, CO_2 is released from benzoic acid or TPA to form benzene, toluene or p-xylene. So, in Figure 4.13, unknown organics reduced significantly from 700 °C to 750 °C, with some compounds cracking. From 750 to 800 °C, benzene kept stable, but biphenyl was improved due to the high temperature. In this temperature range, tar yield does not drop significantly as between 700 and 750 °C, meaning that high temperature cracking is not capable to reduce tar, and secondary tars were promoted a bit. The detailed distribution of 28 species together with unknown between 700 and 800 °C is displayed in Appendix E .

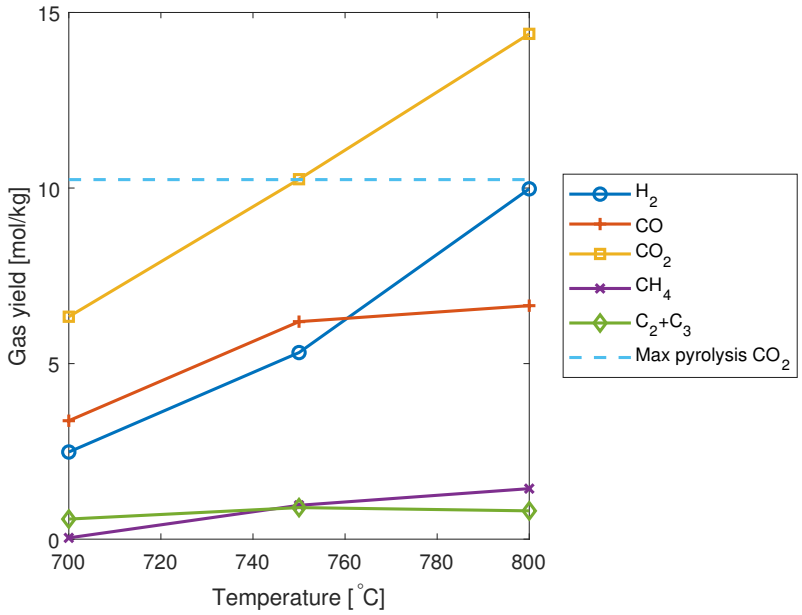

Figure 4.12: The influence of temperature on gas distribution of PET gasification

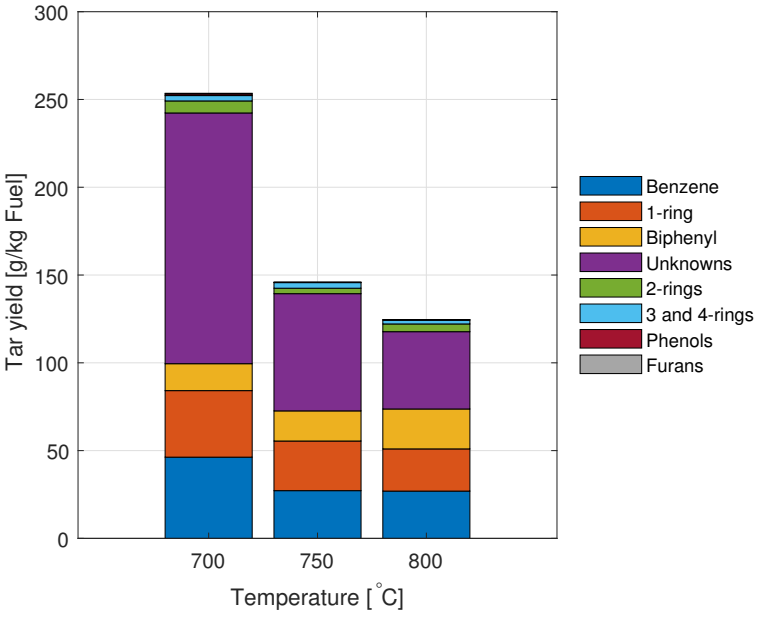

Figure 4.13: The influence of temperature on tar distribution of PET gasification

4.3.2 Residence time

Residence time is defined as the average amount of time that particles stay in the reactor. As Figure 4.14 exhibits, H_2 yield rises slightly, at the same time CO and CO_2

drop a little. Therefore, residence time cannot influence gas yield and distribution a lot. This should be the reason why residence time was not investigated as an essential operational parameter in much research related to plastic gasification. Besides, one of the advantages of the fluidized bed is high efficiency of heat and mass transfer, the residence time cannot affect the extent of the reaction as it does in the fixed bed reactor.

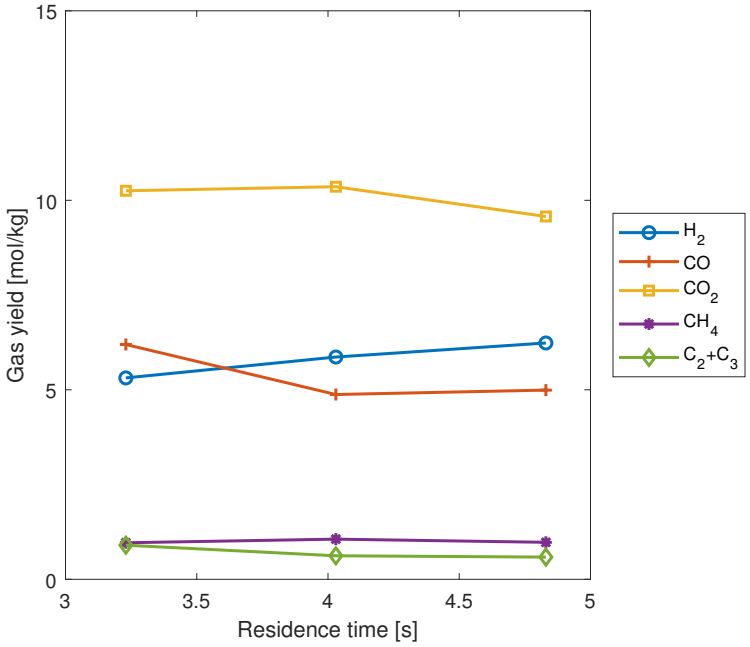

Figure 4.14: The influence of residence time on gas distribution of PET gasification

As Figure 4.15 reveals, the prolonged residence time is helpful to tar formation, where 1-ring, 2-ring, 3-ring, and unknown aromatics were all increased. Longer residence time improves 2,3,4 rings tars, as 2.5 illustrates. Relatively short residence time should be better to avoid tar formation, and the gas product yield can be affected slightly.

4.3.3 S/F ratio

More steam supply can promote H_2 yield by the reactions of steam reforming of tar (R2), char steam gasification (R8: $C + H_2O \rightleftharpoons H_2 + CO$) and WGS reaction (R14). The formation of CO and decreases due to WGS reaction. The same reaction also infers that CO_2 should be increased, but Figure 4.16 shows the opposite trend. The reason could be explained from the tar distribution in Figure 4.17. Increased steam feeding results in the improvement of unknown products. The condensed water can be seen when collecting the products. This phenomenon suggested steam is excessive for PET steam gasification, other reactions with water such as hydrolysis of PET would happen

or the decomposition of benzoic acid was inhibited by the excessive steam.

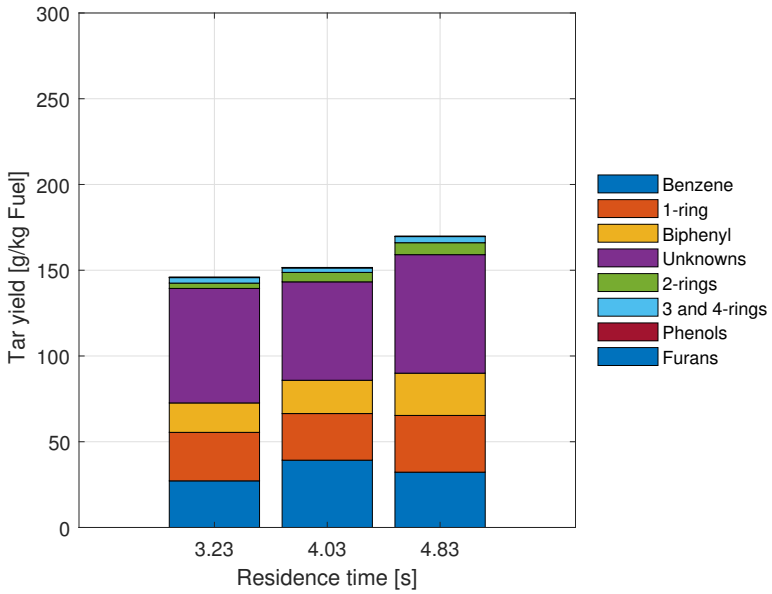

Figure 4.15: The influence of residence time on tar distribution of PET gasification

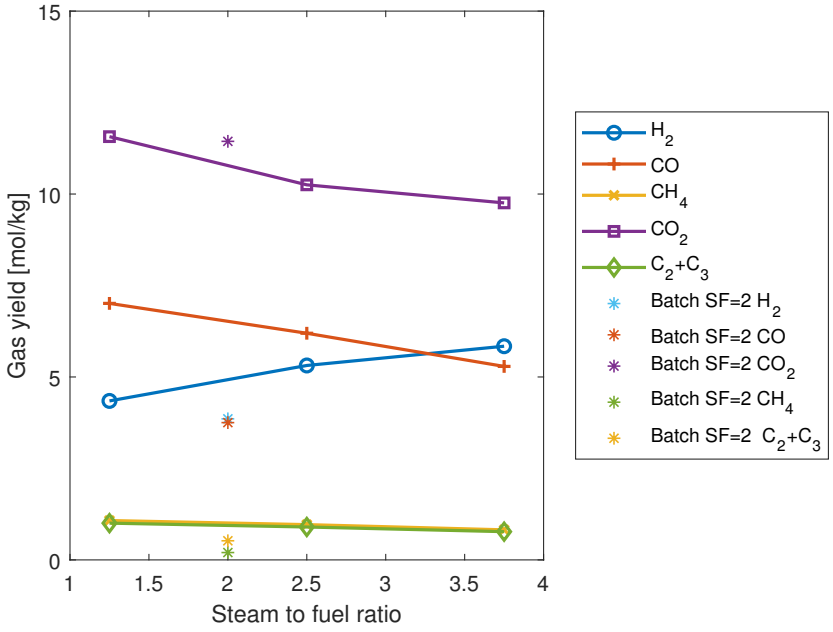

Figure 4.16: The influence of S/F ratio on gas distribution of PET gasification

The scattered points with stars were VPET batch experiment data at the same residence time and temperature. Due to the different steam to fuel ratio between batch (SF=2) and continuous (SF=2.5), the results of them cannot be compared directly. Thus, the results of the batch were scattered in this figure. The continuous feeding experiment can produce more gaseous products, excluding CO_2. The reason is that continuous feeding provides longer time for char gasification reactions. The tar yield in batch experiment has a different magnitude from the continuous feeding experiment. The total tar yield of continuous experiment is around 100 - 300 g/kg fuel which is close to the values in [24, 50, 54]. The reason might be the filter in the syringe that was used in the batch experiment did not absorb the tar effectively.

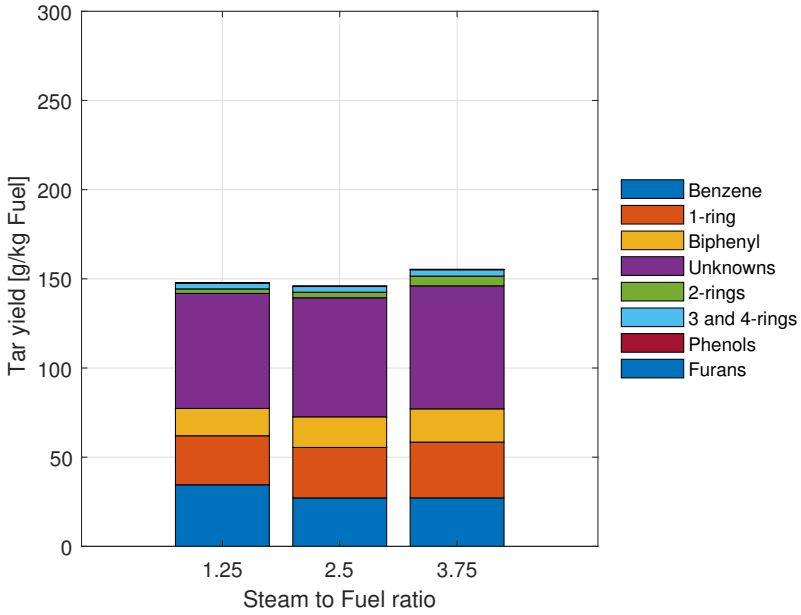

Figure 4.17: The influence of S/F ratio on tar distribution of PET gasification

4.3.4 Continuous feeding bed performance

The temperature and pressure profile along the fluidized bed height are depicted in Figure 4.18. The negative value of height means that the wind box region is below the bed. The profile is from one of the recorded instant values in the case of 750°C, residence time: 4.8s and SF is 2.5. The fluidized gas was introduced from wind box to the bed, where the pressure is 1.7 kPa higher than atmospheric pressure. The pressure drop of the distributor is around 1 kPa. The pressure is stable around atmospheric pressure when the height is higher than MP5, meaning that the region over MP5 (31.65cm) belongs to the freeboard.

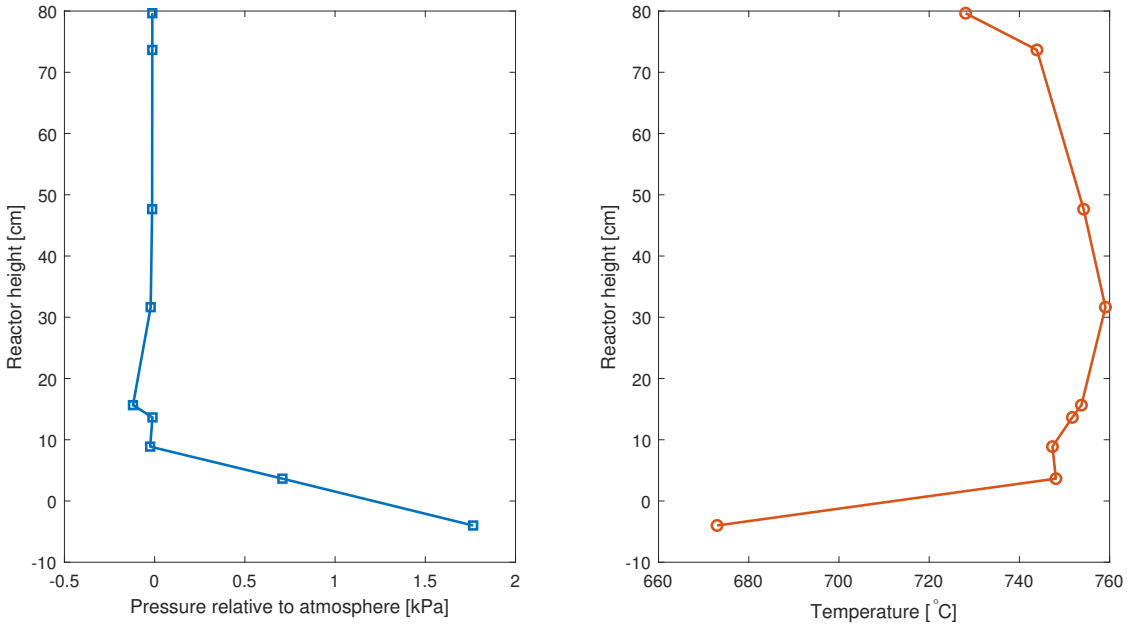

Figure 4.18: The temperature and pressure profiles along the fluidized bed

The temperature distribution along the bed height changed a lot: the temperature of wind box is much lower since fluidized gas is supplied at low temperature (N_2: 20°C, steam: 190°C). MP7 and MP8 are closed to the outlet, so their temperatures were lower than what was set. Temperature increased from MP2 to MP5 and at MP6 dropped slightly. Also, feeding from the top of the reactor could be a problem. Black carbon was observed in the feeding system, which attached on the surface of VPET particles. The loss of carbon can reduce the yield of the product. This phenomenon also indicates that char did not completely reacted.

4.3.5 Mass balance

C, H and O distributions are crucial to the influence of operation conditions analysis in previous sections, and the utilization of products in the next chapter. From Table 3.1, 1 kg PET contains 52 $mol\ C$, 46 $mol\ H$ and 21 $mol\ O$ can be obtained. Then, the ratio of C, H and O between products and PET were computed. Figure 4.19 describes the C, H and O distribution in syngas (CO + H_2), CO_2, hydrocarbons, known tars, unknown tars formed by PET steam gasification at different temperatures, S/F : 2.5 and residence time: 3.23s. The unknown tars were estimated based on the average of molecular weight and carbon number of their adjacent known tars in the calibration.

Carbon balance ratio indicates the conversion efficiency from PET to products. In

all cases, 35% - 40% of C cannot be measured by applied methods, and a large number of tar spcies were not defined. The increasing temperature enhances C in CO_2, CO, HC, and promoting detectable products. The dominant C was formed CO_2 at 800 °C, while at 700 °C, unknown tars had the most carbon. From 700 to 750 °C, the carbon distribution changed significantly, because tar generation dropped dramatically (from 39% to 22%), and CO_2 was improved (from 12% to 20%). At 800 °C, only 13% of C was converted into CO, which is the aim product of carbon conversion in gasification process.

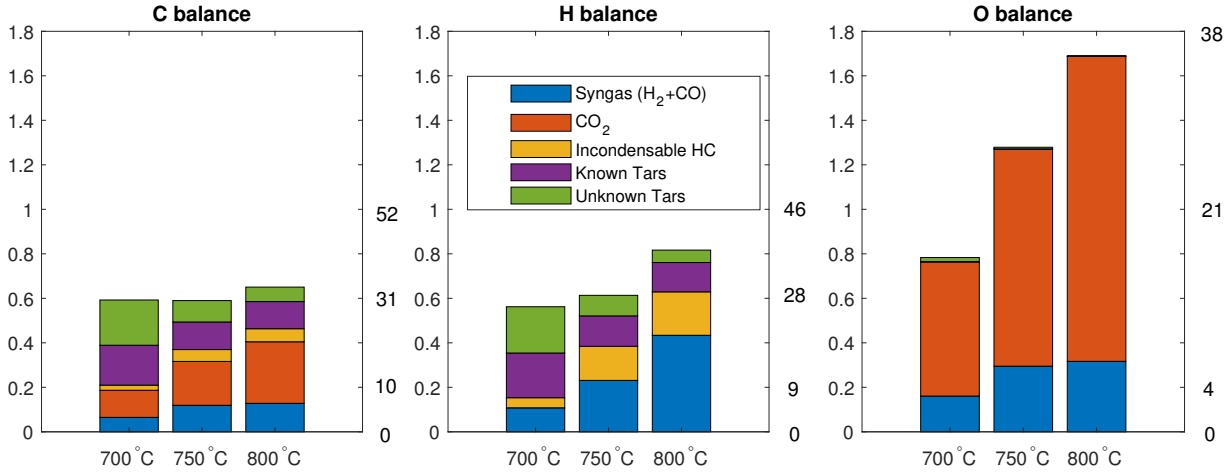

Figure 4.19: C, H and O distribution in products at different temperatures (The left axis: conversion ratio (mol/mol), right axis: C, H, O in (mol/kg PET)

The carbon in form of char was estimated by TGA results at 50 °C/min, where fixed carbon generated by pyrolysis accounts 11.44%. Therefore, in BFB after pyrolysis, the char should be much lower than

$$\frac{1kg \times 1000 \times 11.44\% \times 62.5\%}{12g/mol} \times 100\% = 5.8mol/kgPET \tag{4.7}$$

where 62.5% is the average C wt% composition in PET (see in Table 3.1).

H_2 yield doubled if temperature increased by 50 °C, but H in H_2 was converted from PET or steam can be calculated by O balance. O in products exceeded that should be contained in the feedstocks at 750 and 800 °C. It is assumed that all the exceeded O was converted by steam (although it is known that some oxygen was released from the bed), and the estimation of missing substances, maximum steam conversion (the ratio between reacted steam and total amount of steam) and H from steam to H_2 were shown in Table 4.4.
The ratio of O between product and PET at 700 °C was less than 1, so it is hard to compute the amount of steam reactions. At 750 and 800 °C, less 10% of introduced

Table 4.4: Mass balance analysis

Temperature (°C)	Missing species H/C Ratio	Maximum steam conversion (%)	Maximum H from steam to H_2 (%)
750	1.8	4.1	92
800	2.0	10.4	69

steam took part in the reactions. At 750 °C, maximum 92% of reacted steam was converted into H_2 , which was reduced to 69% at 800 °C. The remained 31% involved in other reactions without producing H_2.

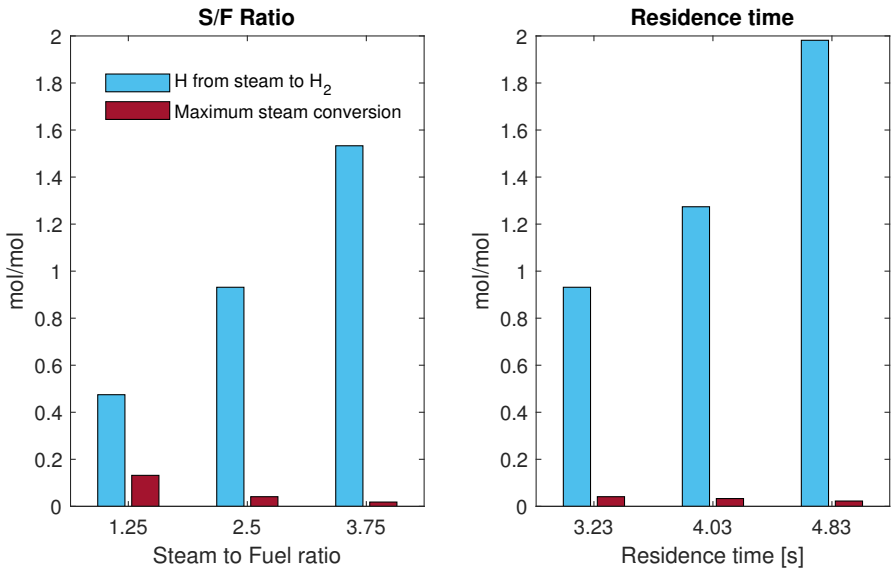

Figure 4.20: Maximum steam conversion and H from steam to H_2 at different SF ratio and residence time

The H/C of missing species were obtained based on the assumption that 5 *mol* fixed carbon was not converted at 750 °C. From table 4.4, it seemed that fixed carbon was converted almost completely at 800 °C, otherwise the ratio is higher than 2, meaning that most missing species were alkane. However, no alkanes with more than 3 carbons were detected at 800 °C. The values infer the main missing species belong to acetaldehyde or cyclic organics without benzene rings, like 1,4-dioxane ($C_4H_8O_2$ 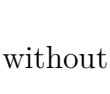) produced by PET pyrolysis [29]. Figure 3.4 also indicated these undetected C could form soot.

Similar analysis of other conditions were conducted. The maximum steam conversion and maximum H from steam to H_2 are depicted in Figure 4.20. The values of H from steam to H_2 higher than 1 suggest H in PET participated H_2 formation and the figure shows more steam and longer residence motivates this conversion of H from PET to H_2. However, introducing more steam into the system promoted the unknown tars or species and reduced the yield of CO_2. Therefore, the maximum steam conversion dropped with increasing steam in this figure, which is opposite to the analysis in 4.3.3.

5

Syngas Application Evaluation and Production Suggestions

In this chapter, the main syngas application: heat and power generation, as well as fuel production will be evaluated based on the results from chapter 4. Some performance parameters and analysis tools would be introduced before the evaluation. Moreover, the suggestions of PET gasification can be proposed.

5.1 Heat and power generation

The parameter of evaluation of the application of heat and power generation is the lower heating value (LHV) of gas product mixture produced by $1kg$ PET steam gasification and cold gas conversion efficiency. Table 5.1 lists LHV of individual gas component and the feedstocks.

Table 5.1: LHV of syngas component, PET and steam [84, 85]

Syngas component (kJ/mol)							Feedstock (kJ/kg)	Agent (kJ/kg)
H_2	CO	CH_4	C_2H_4	C_2H_6	C_2H_2	C_3H_x	PET	Steam (at 190 °C)
242	283	803	1323	1429	1257	1926	21850	2851

The syngas LHV can be calculated by Equation 5.1

$$LHV_{syngas} = \Sigma n_i \cdot LHV_i \tag{5.1}$$

And, CGEE is expressed as Equation 5.2.

$$CGEE = \frac{LHV_{syngas}}{LHV_{PET} + Steam} \tag{5.2}$$

In batch experiment, the char reaction does not complete in 2 min. Therefore, it is difficult to compare the energy conversion efficiency, and only continuous reaction results are provided in this section. In steam gasification, how does different operational parameters influence the heating value? Figure 5.1 describes the LHV and the CGEE of each operational condition. Only reacted steam was considered in the energy calculation based on the results from.

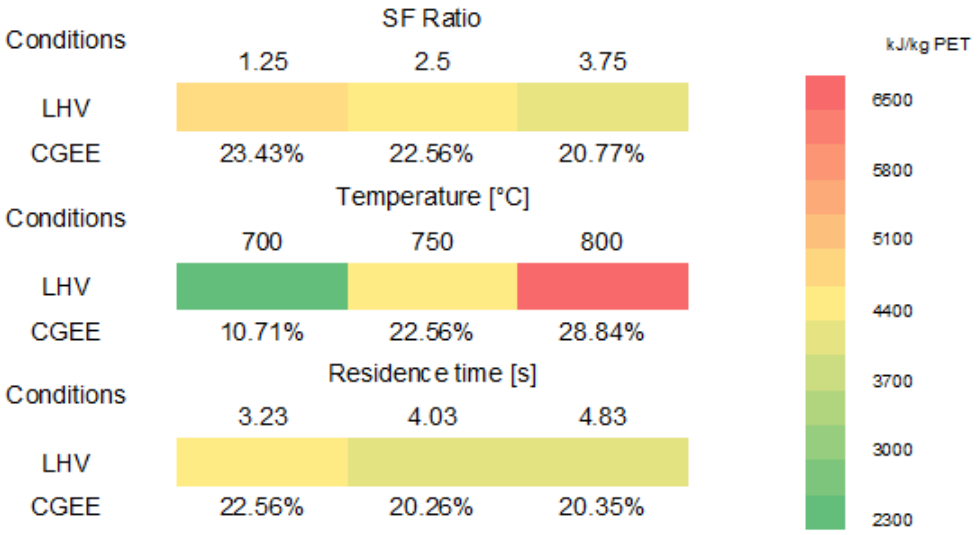

Figure 5.1: The influence of operational parameters on LHV of syngas produced by VPET steam gasification

In this figure, the intensity of the color indicates the LHV of the syngas produced at certain operational conditions. The red color stands for higher LHV. Therefore, the syngas with highest LHV is generated at 800 °C, with the value of 6516 kJ/kg PET. When it is converted to LHV in MJ/m^3 syngas, the value is 8.67 MJ/m^3. The second highest LHV is produced by low S/F ratio, meaning that lower steam supply and lower required energy to heat steam can produce more high LHV gas, such as CO and HC. Although in Figure 4.16, the yields of CH_4 and C_2+C_3 do not drop significantly, their LHVs are very high, especially C_3H_x can hardly be found in the gas product formed at S/F ratio of 3.75. Residence time does not influence the LHV significantly because of the slight effect on gas production distribution.

The highest cold gas conversion efficiency in all cases is 28.84%. Since the boiler does not have specific tar limitation as gas turbine and internal combustion engine, the syngas contained tars can be combusted in the boiler to generate heat and power. Figure 5.2 the conversion efficiency when tar is also considered. All the tar components are classified as light tar (Molecular Weight $\geq$ 200) with the average LHV of 39420 kJ/kg, since only a few tars in the products belong to heavy tar. When tar is included as the combustible fuel, the conversion efficiency in all cases increased to about 50%, in which 700 °C converted the most heat energy from PET to the product. The efficiency was improved from the lowest one, 11% to the highest, 58%.

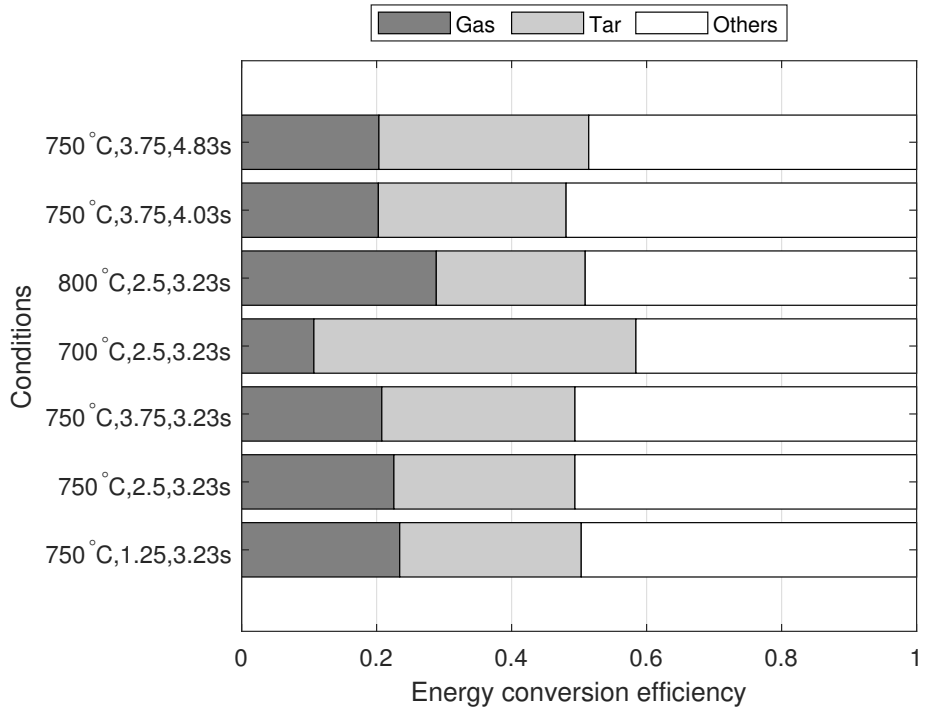

Figure 5.2: The influence of operational parameters on LHV of syngas and tars produced by VPET steam gasification

5.2 Fuel synthesis

Another application of syngas is to produce fuels, where the ratio between H_2 and CO as well as tar content should be paid attention to. The function of CO_2 in fuel synthesis is still debated. In most cases, CO_2 can inhibit the catalytic reaction of H_2 and CO synthesis. CO_2 should be removed in the product cleaning system.

Based on the data in Table 2.9, a coordinate system is established. X and Y axis represent the yield of CO and H_2, respectively. The slope of the straight line is equal to H_2/CO, as Figure 5.3 shows. The zones and lines symbolize different H_2/CO ratio for various fuel products. For example, the points in zones VII and VIII can be used to produce the fuel of hydrogen, and Table 5.2 lists the lines and zones for all fuel synthesis applications.

Figure 5.4 illustrates the locations of all batch experiment in the fuel synthesis zones. As it suggests, syngas produced by VPET pyrolysis, RPET pyrolysis, and VPET air gasification cannot be used for any fuel synthesis process because none of their H_2/CO

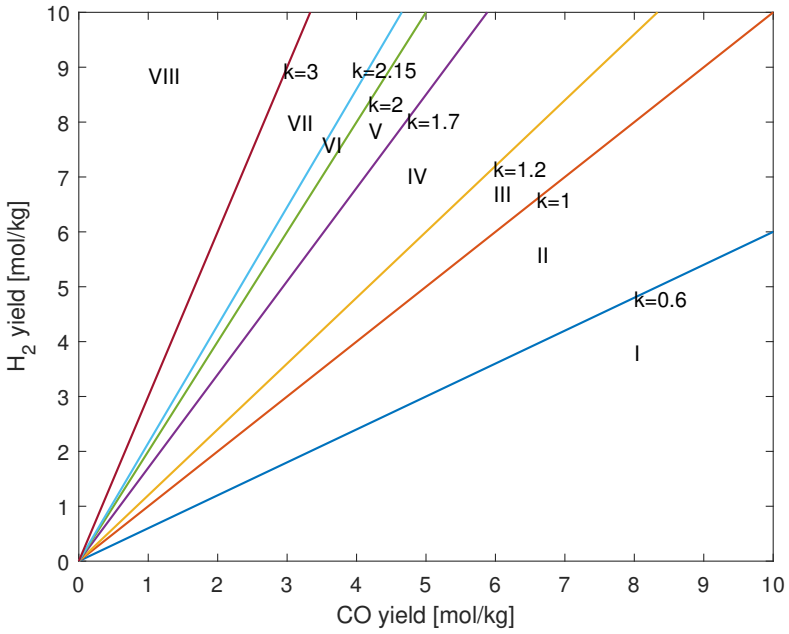

Figure 5.3: H_2/CO profiles for fuel synthesis from syngas

Table 5.2: The zones and lines of each fuel synthesis application

	Methanol	Ethanol	DME	FTS	Hydrogen	SNG
Zones or lines	k=2,k=3	k=2,Zone III	Zone around k=1 and k=2, k=3	Zones II+III+IV, k=2,Zone VI	Zones VII+VIII	Zone VIII

ratio can reach the minimum value for fuel synthesis. Syngas generated from VPET steam gasification, RPET steam gasification, VPET air gasification, and PE pyrolysis are in the zone of FTS production, at the pressure of 10-40 *bar*, and H_2/CO_2 must be kept as 1. The H_2/CO of VPET steam gasification, and VPET air with steam gasification products are approximately 1, so, they can produce DME at the same condition with methanol synthesis but with additives. The H_2/CO of PE steam gasification is over 5, which is ideal for SNG and hydrogen production.

Figure 5.5 reveals the locations of syngas produced at different operational parameters in the fuel synthesis zones. All the cases are suitable to synthesis FTS, in which H_2 and CO produced in longer residence time as well as the highest S/F ratio are in the range of ethanol synthesis assisted by MoS_2 at 70-105 *bar*. No operational conditions can

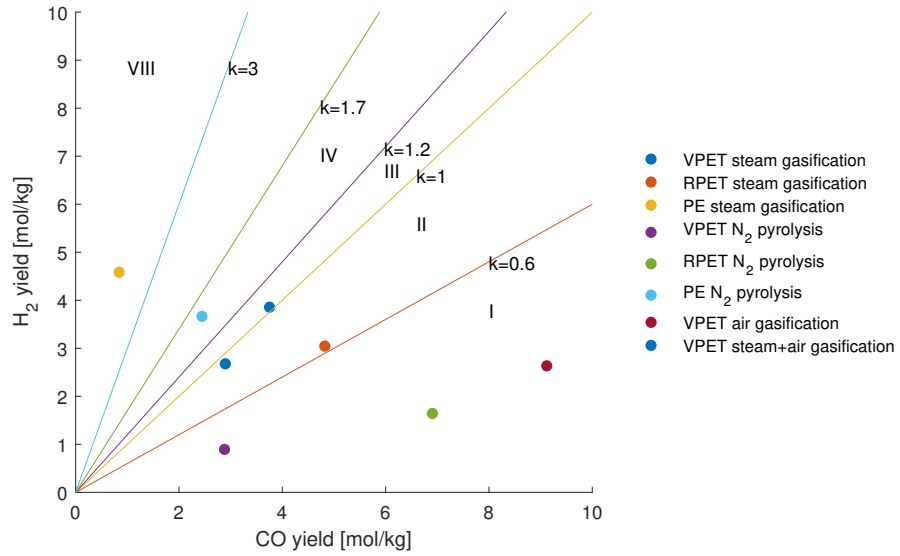

Figure 5.4: The locations of all batch experiment in the fuel synthesis zones

help PET gasified syngas reach the H_2/CO ratio to 2, which means methanol cannot be the direct product for these syngas products. If methanol is the aim product, water gas shift reactor may be the way forward.

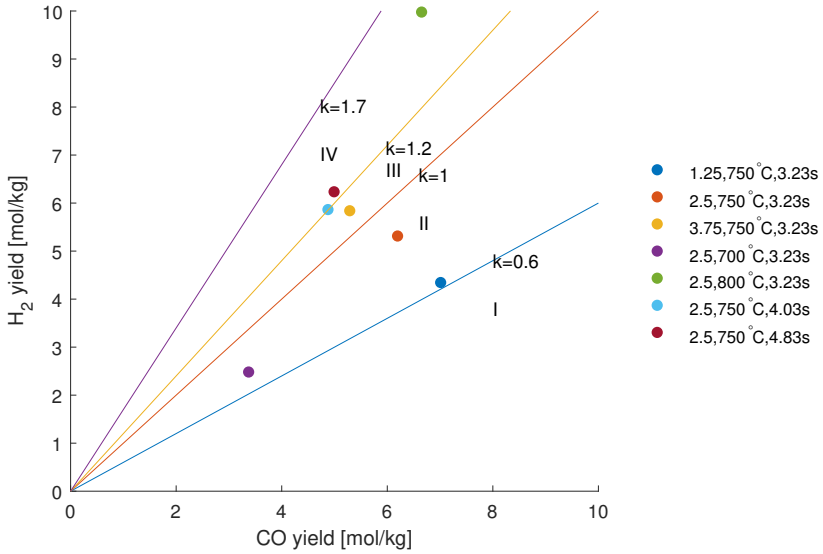

Figure 5.5: The locations of all continuous experiments in the fuel synthesis zones

5.3 Fuel production suggestions

The previous analysis shows that the application of PET gasification syngas product is so narrow. However, PET is commonly used in daily life. Gasification should be a potential recycling approach to reuse PET to produce energy and fuels. Therefore, some strategies should be put forward to extend PET gasification syngas application, in terms of feedstocks, operational conditions, catalysts and tar removal.

5.3.1 Operational conditions

The influence of temperature, residence time, and S/F ratio on gas production distribution has been discussed in Chapter 4. One question should be solved: which condition affect the gas production distribution and performance parameters most? The answer to this question can give a clue to enhance the performance of the product significantly by a slight change of operating conditions. Due to the various scale of values and units, the average and standard deviation cannot be used to compare the variation of each parameter. In statistics, a dimensionless number, coefficient of variation (C_v) permits the comparison free of scale effects and it is performed as Equation 5.3 [86].

$$C_v = \frac{\sigma}{\bar{\mu}} \tag{5.3}$$

where, σ is the standard deviation and $\bar{\mu}$ is the mean of a series of data.

In this project, the aim of introducing the concept of coefficient of variation is to measure if the condition parameter can result in a remarkable change of performance. The high value, in this case, means that this is a critical parameter for PET steam gasification, which is beneficial to optimize the operational conditions so that the gas yield can be improved.

The influence extent of operational conditions on syngas component is displayed in Figure 5.6. The influence extent can be roughly sorted as Temperature > steam to fuel ratio > residence time, as discussed in the previous chapter. However, for C_2+C_3, residence time can influence more than temperature and S/F ratio. That is because longer residence time can be helpful for the formation of small molecule HC. Also, due to their values are minimal, minor fluctuations can cause the factor to be higher. Actually, temperature affects the distribution of C_2H_4, C_2H_6, C_2H_2, C_3H_x but the total amount does not fluctuate as severely as residence time.

The influence extent of operational conditions on tar distribution is shown in Figure 5.7. Temperature is still the essential parameter for each tar species, especially furans and phenols; the σ values are over 1. This indicates that temperature can affect the

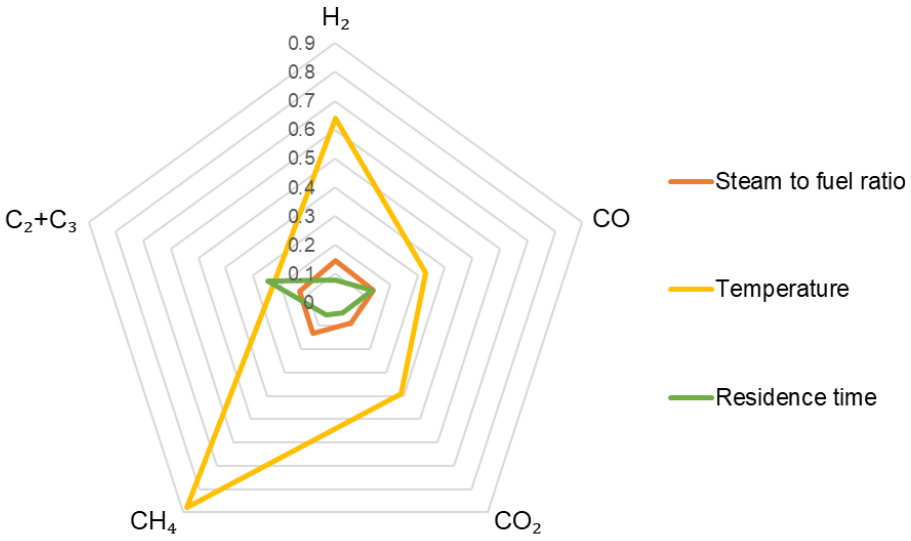

Figure 5.6: The influence extent of operational conditions on syngas component

formation or decomposition of furans and phenols significantly, especially from 700 to 750 °C, a remarkable dropping of furans and phenols can be observed. Residence time plays the second most important role in operational conditions; then SF ratio cannot influence all types of tar so much.Temperature and residence time are essential parameters for multiple ring tars formation, therefore, their influence extent on 2,3,4 rings tars were almost same.

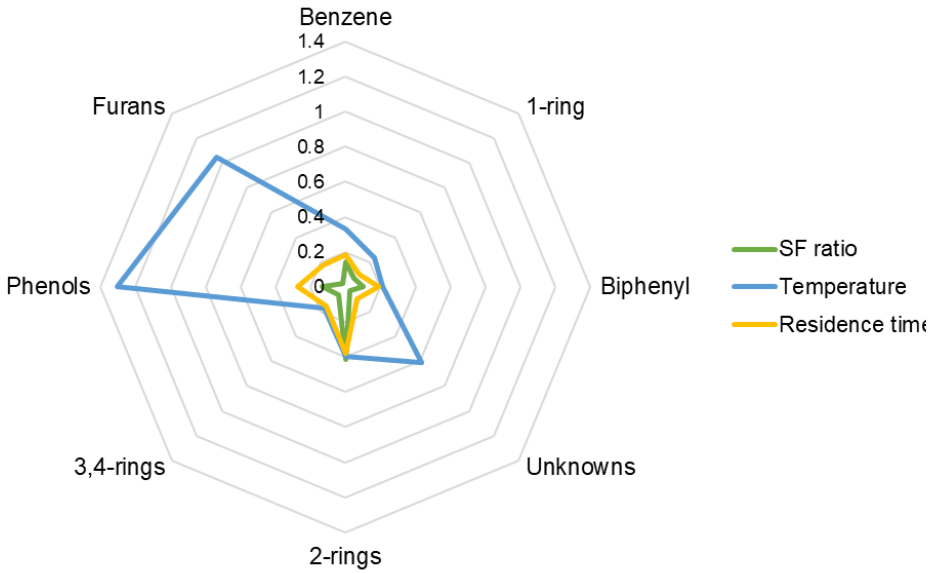

Figure 5.7: The influence extent of operational conditions on tar component

H_2/CO ratio, LHV, and Tar concentration are three essential parameters for syngas production assessment. The influence of the operational conditions on these parameters is depicted in Figure 5.8. Temperature is still the critical operational parameter for H_2/CO ratio, LHV, and Tar concentration where LHV is affected by temperature the most. For tar formation, as mentioned previously, this result does not mean tar can be reduced by high temperature. This remarkable drop only occurs from 700 to 750 °C. Steam to fuel ratio can influence H_2/CO more than residence time while residence time is more important than steam to fuel ratio for tar formation.

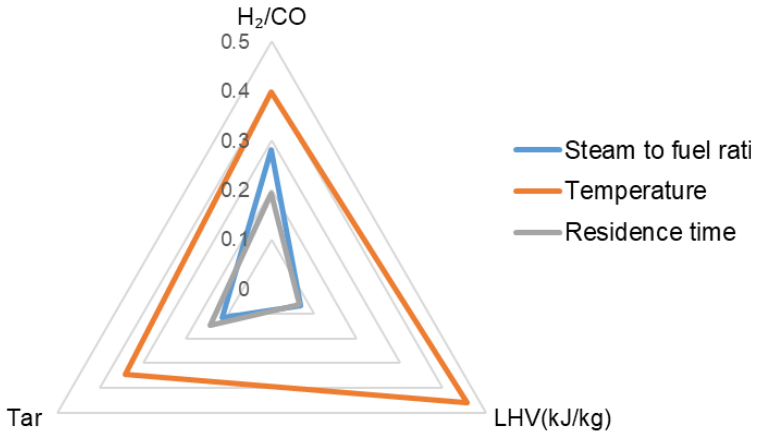

Figure 5.8: The influence extent of operational conditions on evaluation parameters

In Wilk & Hofbauer [54]'s experiment, steam to fuel ratio was set between from 1 to 2, so, the original design in this project was 1 to 3. However, it was tough to search an accurate voltage for the feeding rate of PET as $1g/min$, and the 0.8 was closest value can be found. Therefore, the S/F ratio was changed into 1.25 to $3.75g/min$. If the syngas contains a lot of steam, higher energy should be applied to produce steam and condense the steam in syngas applications. An appropriate S/F ratio must be investigate to keep balance between syngas yield and energy consumption, which can be carried out by a integration modeling.

5.3.2 Plastic mixture as feedstock

The batch results indicate that the H_2/CO ratio of PE steam gasification is much higher than that of VPET gasification. One idea could be gasifying the mixture of PE and PET with a proper proportion. However, according to Wilk & Hofbauer [54]'s result, this idea does not seem so positive to fuel production. Table 5.3 shows the gas composition (vol%) and the H_2/CO molar ratio which is calculated by Equation 4.3.

Since Wilk & Hofbauer did not investigate the pure PET steam gasification, it is hard

Table 5.3: Gas product composition (vol%) from Wilk & Hofbauer's [54] result and H_2/CO molar ratio as well as CGCE

Feedstock	H_2	CO	CO_2	CH_4	C_2H_4	C_xH_y	H_2/CO	CGEE (%)
PE	38	7	8	30	15	2	5.40	76.67
PP	34	4	8	40	12	2	8.45	66.11
PP+PE (50:50)	47	22	5	16	8	2	2.12	48.14
PE+PET (20:80)	27	20	29	15	8	1	1.34	64.80
PE+PS (40:60)	51	23	7	11	7	1	2.20	45.58

to know how the mixture would affect the gas products compared with PET steam gasification. However, from the data of PE, PP and their mixture, both of the gas yield of H_2 and CO increased in which CO surged from 7 vol % to 22 vol %. This result suggests that each component in the plastic mixture can interact with each other to promote the yield of CO and H_2. Nevertheless, due to the booming of CO, H_2/CO ratio is much lower than before. The results in different scale of the reactor cannot be compared directly, but can still provide some hints. In this project result, at 800 °C, the H_2/CO is around 1.5, and the higher the temperature is, the higher H_2/CO can be obtained. Wilk & Hofbauer's experiment was conducted at 850 °C means H_2/CO value could be larger than 1.5. However, H_2/CO was 1.34 in the case of 20:80 PE and PET mixture steam gasification, which is lower than H_2/CO of PE or PET gasified individually. It can be inferred that mixing plastic could not promote the H_2/CO of PET steam gasification, but it is still required to be proved by additional experiments.

The cold gas energy conversion efficiency could be improved when PET and PE mixed. In this project, the energy conversion efficiency of PET steam gasification is very low, up to 40% at the temperature of 800 °C, but the blending of PE and PET can reach 64.80%. Although PE and PP have a very high efficiency on energy conversion, their mixture is even much lower than each of them.The reason is lower concentration of CH_4, C_2H_4, C_xH_y with high LHV. Therefore, the mixture of PET with PE could be effective for syngas combustion.

Wilk & Hofbauer also investigated the tars in different cases, the cases of PE and PE + PET are shown in Table 5.4. In their product of PE + PET gasification production, naphthalene and anthracene account for the most while in this project the sum of them is less than 1%. Biphenyl has a similar value. The total tar concentration shows that the mixture of PE and PET could be helpful to reduce the tar formation, but the conclusion can be obtained by additional experiments.

Table 5.4: Tar composition (vol%) from Wilk & Hofbauer's [54] result at 850 °C and this project at 800°C

			PE	PE +PET	This project
Aromatics	Styrene	wt%	7	9	9.50
	1H indene	wt%	4	4	2.71
Naphthalenes	Naphthalene	wt%	40	26	0.09
PAH	Acenaphthylene	wt%	15	8	0.94
	Anthracene	wt%	14	19	0.15
	Phenanthrene	wt%	4	1	0.62
	Biphenyl	wt%	3	20	17.67
	Pyrene	wt%	3	1	0.07
	Fluorene	wt%	2	1	0.48
Total		g/Nm^3	150	102	138

5.3.3 PET mixed with biomass as feedstock

Burra & Gupta [87] studied biomass steam gasification combined with plastic waste in a semi-batch reactor at 1173K. Wood pellets of 100% pinewood were used to represent biomass and PET was one of the plastic wastes. The fractions of plastics were 0, 60%, 80%, and 100%. The results of gas distribution were illustrated in Table 5.5. In this table, the mass of CO was calculated by the information of CO/CO_2 molar ratio and CO_2 yield. All gaseous hydrocarbon (CH_4 and C_2H_x) were measured altogether. Thus the heating value of the mixture was viewed as that of C_2H_4.

Table 5.5: Gas product composition(g) from Burra & Gupta's result and H_2/CO molar ratio as well as CGCE

Feedstock	H_2	CO	CO_2	C_xH_y	H_2/CO	CGCE (%)
Pinewood	1.3	16.96	19.6	6.2	1.07	93.69
PET+Pinewood (60:40)	1.65	14.25	28	3.4	1.62	71.96
PET+Pinewood (80:20)	1.5	12.47	19.6	2.2	1.68	57.63
PET	1.25	14.97	16.8	1.6	1.17	51.34

In contrast to plastic mixtures, PET co-gasified with biomass can improve both H_2/CO ratio and CGCE, meaning that PET and pinewood promote each other during the steam gasification process. The H_2/CO ratio after blending with pinewood is still in the range of pure PET fuel production applications, but it reveals biomass can enhance

PET steam gasification performance, and other types of biomass can be analyzed to find the best friend for PET co-gasification. The results also show the fraction of blending should be different for combustible gas and fuel production: biomass should dominate if the gaseous product will be burnt to produce heat and power while high PET composition can obtain ideal fuel production raw gas.

5.3.4 By-products utilization

As it was calculated in 4.3.5, 42% of C at 800 °C cannot be defined in this experiment. Sampling device and advanced product analysis method must be applied to obtain the details of these unknown substances. For gasification, all of them are by-products. Since 54% C were by-products, these products must be considered how to utilize them. After the determination of all species, the utilization evaluation can be done as the gas product. This section proposes some possible solutions.

As in 4.3.4 mentioned, black carbon can be observed in the feeding system. This should be unreacted char, which accounted for less than 18.33% in total carbon, as the calculation in 4.3.5. Char can be burnt to produce heat for gasification in DFB as Wilk & Hofbauer [54] did. Also, char can be collected and used to remove the heavy metal in water treatment due to their porous structure [6].

Tar formation is remarkable during PET steam process and far from the limitation of any heat production and fuel synthesis process. 99.99% of tar should be removed, which is not developed on the industrial scale. Therefore, the tar removal should be completed by several steps. As Skive Fjernvarme plant mentioned in 2.6.1, a tar reforming unit is required to convert tars into gas product entirely. Feeding position could reduce the formation of tar, which is inspired by Brachi et al [51]. Another solution is to make use of these tars. For instance, the concentration of BTX is very high. If it is possible, BTX can be condensed easily due to the low boiling points, and they can be sold as a by-product to other chemical synthesis processes. At 700 °C, $1kg$ PET can produce $70g$ BTX, but the gas yield is very low. So, the economic performance should be evaluated by further research to obtain a profitable operation condition. The liquid oil product can also be the substitute of gasoline and diesel. This can be assessed by octane and cetane number measurements after the components determination.

5.3.5 Perspective of syngas applications

Maniatis derived the status of syngas applications for market potential and technology reliability, as Figure 5.9 reveals. This figure illustrates that currently, syngas produced by biomass gasification has priority for heat and power generation (except for fuel cell) due to their outstanding techno-economic performance. Therefore, the syngas generated from PET steam gasification is likely to be applied to heat and power generation.

However, the conversion efficiency from PET to syngas is low. The product quality improvement must be carried out. The previous analysis shows temperature can enhance the syngas yield and HHV significantly. Other solutions such as changing bed material and mixed with other plastic or biomass should be proved by further research. Finally, based on these optimal operation conditions, the modeling of integration system is necessary to analyze and optimize the whole system.

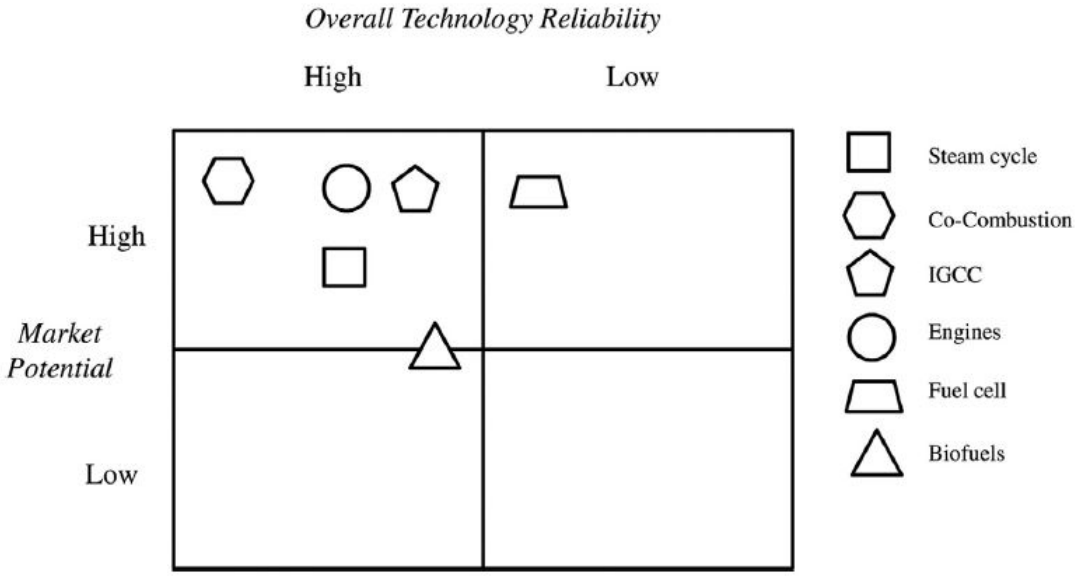

Figure 5.9: The status of syngas applications for market potential and technology reliability [55]

6

Conclusion

This experimental work demonstrates PET is a difficult fuel to be gasified, because the dominant product is CO_2 due to its structure. TGA results revealed that virgin PET contains 11%-15% char, 85%-89% volatile, and a little amount of moisture. RPET has almost the same decomposition curve as virgin PET, but with higher moisture and volatile. The heating rate can affect how fast the main weight loss before the specific value, after this heating rate, the TGA curves in the period of main weight loss will coincide with each other. This fact infers that devolatilization process at the heating rate of 50 $°C/min$ would be similar to the much higher heating rate in bubbling fluidized bed.

Batch experiments compared different plastics and gasifying agents. Although TGA illustrated VPET and RPET have similar curves, their products generated by pyrolysis and gasification were different. Besides, PET produces a large amount of CO_2 in the air. Steam can motivate PET to generate H_2, but the effect is not as same as air for CO_2.

Continuous feeding experiments investigated the influence of temperature, residence time, and steam/fuel ratio for PET steam gasification. Among these three operational conditions, temperature affects the product distribution more than residence time and steam/fuel ratio. Higher temperature can motivate the gas yield and tar cracking. However, prominent tar cracking occurred from between 700 and 750 °C and high temperature induce the formation of multiple rings aromatic that is hard to remove. Higher residence time and steam/fuel ratio are also positive to produce tars, although both of them can improve H_2 yield. However, the mass balance results indicated that, at 800 °C, approximate 13% of carbon in PET was converted into CO, and around 69% of reacted steam was converted into H_2.

Based on the results, the application of syngas was evaluated. Because of the high content CO_2, carbon capture unit is required for both applications. For the heat and power production, higher temperature can improve the cold gas energy efficiency to 29%. Even the heat in tar is considered, the highest efficiency is only 58%. Most cases of H_2/CO meet the requirement of the FTS process, some of them can be used to produce DME and ethanol. PET steam gasification produces high concentration tars, which can prevent the syngas applications, further tar cracking and reforming process is required, or recover tars as a by-product. At present, biomass gasification integrated with heat and power production performs well in market potential and technology relia-

bility. So heat and power generation should be the prior application of syngas produced by PET steam gasification.

This collecting and analysis method in this experiment should be improved in the future. In the carbon balance, 35% to 40% of C cannot be measured, which weakens the analysis of further application analysis. The unknown tars also must be defined, in which, TPA and benzoic acid are crucial to analyze the whole process and applications. Besides, the oxygen in the bed increased the yield of CO and CO_2, so N_2 should be introduced into the system for a longer time to purge the air as much as possible. Then, more accurate process analysis and product application evaluation can be proposed.

Extra work should be done for the syngas product applications since high CO_2 and tar yield can inhibit syngas applied to both heat production and fuel synthesis. First, the influence of bed material should be tested to search for a suitable bed material to improve tar cracking and H_2 yield. Another solution is to mix PET with other plastics or biomass. Researchers have done this job, but none of them showed the results compared with PET steam gasification. PET mixed with other plastics or biomass for steam gasification should be investigated to improve the performance of PET steam gasification. Afterward, with these experimental results, modeling of PET steam gasification integrated with either heat production or fuel synthesis can be established to analyze the technical and economic performance of the whole system, including the mass balance, energy and exergy balance as well as the cost and profit.

References

[1] Lopez, G., Artetxe, M., Amutio, M., Alvarez, J., Bilbao, J., Olazar, M. (2018). Recent advances in the gasification of waste plastics. A critical overview. Renewable and Sustainable Energy Reviews, 82, 576-596.

[2] Kunwar, B., Cheng, H. N., Chandrashekaran, S. R., Sharma, B. K. (2016). Plastics to fuel: a review. Renewable and Sustainable Energy Reviews, 54, 421-428.

[3] Plastics – the Facts 2018. An analysis of European plastics production, demand and waste data; 2018

[4] Geyer, R., Jambeck, J. R., Law, K. L. (2017). Production, use, and fate of all plastics ever made. Science advances, 3(7), e1700782.

[5] Al-Salem, S. M., Lettieri, P., Baeyens, J. (2009). Recycling and recovery routes of plastic solid waste (PSW): A review. Waste management, 29(10), 2625-2643..

[6] Sharuddin, S. D. A., Abnisa, F., Daud, W. M. A. W., Aroua, M. K. (2016). A review on pyrolysis of plastic wastes. Energy conversion and management, 115, 308-326.

[7] Marco, I. D., Caballero, B., Torres, A., Laresgoiti, M. F., Chomon, M. J., Cabrero, M. A. (2002). Recycling polymeric wastes by means of pyrolysis. Journal of Chemical Technology Biotechnology: International Research in Process, Environmental Clean Technology, 77(7), 817-824.

[8] Klinghoffer, N. B., Castaldi, M. J. (2013). Gasification and pyrolysis of municipal solid waste (MSW). In Waste to Energy Conversion Technology (pp. 146-176).

[9] Pereira, E. G., da Silva, J. N., de Oliveira, J. L., Machado, C. S. (2012). Sustainable energy: a review of gasification technologies. Renewable and sustainable energy reviews, 16(7), 4753-4762.

[10] Higman, C. (2016). State of the gasification industry: Worldwide gasification and syngas databases 2016 update. Available at www. gasification-syngas. org/uploads/downloads/2016-presentations/2016-Wed-Higman. pdf. Accessed June, 8, 2017.

[11] Thomas, S., Visakh, R. M. (2011). Handbook of Engineering and Speciality Thermoplastics: Polyethers and Polyesters, Vol. 3. Canada: Scrivener Publishing (pp. 97-126).

[12] Nikles, D. E., Farahat, M. S. (2005). New motivation for the depolymerization products derived from poly (ethylene terephthalate)(PET) waste: A review. Macromolecular Materials and Engineering, 290(1), 13-30.

[13] Olabisi, O., Adewale, K. (2016). Handbook of thermoplastics. CRC press (pp. 319-346).

[14] Göschel, U. (2005). Handbook of Thermoplastic Polymers: Homopolymers, Copolymers, Blends, and Composites.

[15] https://www.beroeinc.com/whitepaper/pet-recycle/

[16] Bach, C., Dauchy, X., Chagnon, M. C., Etienne, S. (2012). Chemical compounds and toxicological assessments of drinking water stored in polyethylene terephthalate (PET) bottles: a source of controversy reviewed. Water research, 46(3), 571-583.

[17] Kutz, M. (Ed.). (2017). Applied plastics engineering handbook: processing and materials (2nd Edition). William Andrew.

[18] Sinha, V., Patel, M. R., Patel, J. V. (2010). PET waste management by chemical recycling: a review. Journal of Polymers and the Environment, 18(1), 8-25.

[19] Al-Sabagh, A. M., Yehia, F. Z., Eshaq, G., Rabie, A. M., ElMetwally, A. E. (2016). Greener routes for recycling of polyethylene terephthalate. Egyptian Journal of Petroleum, 25(1), 53-64.

[20] Jankauskaite, V., Macijauskas, G., Lygaitis, R. (2008). Polyethylene terephthalate waste recycling and application possibilities: a review. Mater Sci (Medžiagotyra), 14(2), 119-127.

[21] Shen, L., Worrell, E., Patel, M. K. (2010). Open-loop recycling: A LCA case study of PET bottle-to-fibre recycling. Resources, conservation and recycling, 55(1), 34-52.

[22] Komly, C. E., Azzaro-Pantel, C., Hubert, A., Pibouleau, L., Archambault, V. (2012). Multiobjective waste management optimization strategy coupling life cycle assessment and genetic algorithms: Application to PET bottles. Resources, conservation and recycling, 69, 66-81.

[23] Chilton, T., Burnley, S., Nesaratnam, S. (2010). A life cycle assessment of the closed-loop recycling and thermal recovery of post-consumer PET. Resources, Conservation and Recycling, 54(12), 1241-1249.

[24] Basu, P. (2018). Biomass gasification, pyrolysis and torrefaction: practical design and theory. Academic press.

[25] Higman, Christopher van der Burgt, Maarten. (2008). Gasification (2nd Edition). Elsevier.

[26] Mahinpey, N., Gomez, A. (2016). Review of gasification fundamentals and new findings: reactors, feedstock, and kinetic studies. Chemical Engineering Science, 148, 14-31.

[27] Pütün, A. E., Apaydin, E., Pütün, E. (2002). Bio-oil production from pyrolysis and steam pyrolysis of soybean-cake: product yields and composition. Energy, 27(7), 703-713.

[28] Duman, G., Yanik, J. (2017). Two-step steam pyrolysis of biomass for hydrogen production. International Journal of Hydrogen Energy, 42(27), 17000-17008.

[29] Levchik, S. V., Weil, E. D. (2004). A review on thermal decomposition and combustion of thermoplastic polyesters. Polymers for Advanced Technologies, 15(12), 691-700.

[30] Montaudo, G., Puglisi, C., Samperi, F. (1993). Primary thermal degradation mechanisms of PET and PBT. Polymer degradation and stability, 42(1), 13-28.

[31] Brems, A., Baeyens, J., Beerlandt, J., Dewil, R. (2011). Thermogravimetric pyrolysis of waste polyethylene-terephthalate and polystyrene: A critical assessment of kinetics modelling. Resources, Conservation and Recycling, 55(8), 772-781.

[32] FakhrHoseini, S. M., Dastanian, M. (2013). Predicting pyrolysis products of PE, PP, and PET using NRTL activity coefficient model. Journal of Chemistry, 2013.

[33] Çepelioğullar, Ö., Pütün, A. E. (2013). Utilization of two different types of plastic wastes from daily and industrial life. Journal of Selcuk University Natural and Applied Science, 2(2), 694-706.

[34] Artetxe, M., Lopez, G., Amutio, M., Elordi, G., Olazar, M., Bilbao, J. (2010). Operating conditions for the pyrolysis of poly-(ethylene terephthalate) in a conical spouted-bed reactor. Industrial Engineering Chemistry Research, 49(5), 2064-2069.

[35] Dimitrov, N., Krehula, L. K., Siročić, A. P., Hrnjak-Murgić, Z. (2013). Analysis of recycled PET bottles products by pyrolysis-gas chromatography. Polymer degradation and stability, 98(5), 972-979.

[36] Yoshioka, T., Grause, G., Eger, C., Kaminsky, W., Okuwaki, A. (2004). Pyrolysis of poly (ethylene terephthalate) in a fluidised bed plant. Polymer Degradation and Stability, 86(3), 499-504.

[37] Saad, J. M., Williams, P. T. (2016). Pyrolysis-catalytic-dry reforming of waste plastics and mixed waste plastics for syngas production. Energy Fuels, 30(4), 3198-3204.

[38] Milne, T. A., Evans, R. J., Abatzaglou, N. (1998). Biomass Gasifier"Tars": Their Nature, Formation, and Conversion (No. NREL/TP-570-25357; ON: DE00003726). National Renewable Energy Laboratory, Golden, CO (US).

[39] Abu El-Rub, Z., Bramer, E. A., Brem, G. (2004). Review of catalysts for tar elimination in biomass gasification processes. Industrial engineering chemistry research, 43(22), 6911-6919.

[40] Rios, M. L. V., González, A. M., Lora, E. E. S., del Olmo, O. A. A. (2018). Reduction of tar generated during biomass gasification: A review. Biomass and bioenergy, 108, 345-370.

[41] Anis, S., Zainal, Z. A. (2011). Tar reduction in biomass producer gas via mechanical, catalytic and thermal methods: A review. Renewable and sustainable energy reviews, 15(5), 2355-2377.

[42] Speight, J. G. (2014). Gasification of unconventional feedstocks. Gulf Professional Publishing.

[43] Basu, P. (2006). Combustion and gasification in fluidized beds. CRC press.

[44] Elnashaie, S. S., Danafar, F., Rafsanjani, H. H. (2015). Nanotechnology for chemical engineers. Springer.

[45] Scala, F. (Ed.). (2013). Fluidized bed technologies for near-zero emission combustion and gasification. Elsevier.

[46] Yates, J. G., Lettieri, P. (2016). Fluidized-bed reactors: processes and operating conditions (Vol. 26). Springer.

[47] Arena, U., Mastellone, M. L. (2000). Defluidization phenomena during the pyrolysis of two plastic wastes. Chemical Engineering Science, 55(15), 2849-2860.

[48] Brems, A., Baeyens, J., Beerlandt, J., Dewil, R. (2011). Thermogravimetric pyrolysis of waste polyethylene-terephthalate and polystyrene: A critical assessment of kinetics modelling. Resources, Conservation and Recycling, 55(8), 772-781.

[49] Robinson, T., Bronson, B., Gogolek, P., Mehrani, P. (2016). Comparison of the air-blown bubbling fluidized bed gasification of wood and wood–PET pellets. Fuel, 178, 263-271.

[50] Pohořelý, M., Vosecký, M., Hejdová, P., Punčochář, M., Skoblja, S., Staf, M., ... Svoboda, K. (2006). Gasification of coal and PET in fluidized bed reactor. Fuel, 85(17-18), 2458-2468.

[51] Brachi, P., Chirone, R., Miccio, F., Miccio, M., Picarelli, A., Ruoppolo, G. (2014). Fluidized bed co-gasification of biomass and polymeric wastes for a flexible end-use of the syngas: focus on bio-methanol. Fuel, 128, 88-98.

[52] Kraft, S., Kirnbauer, F., Hofbauer, H. (2018). Influence of drag laws on pressure and bed material recirculation rate in a cold flow model of an 8 MW dual fluidized bed system by means of CPFD. Particuology, 36, 70-81.

[53] Koppatz, S., Pfeifer, C., Rauch, R., Hofbauer, H., Marquard-Moellenstedt, T., Specht, M. (2009). H2 rich product gas by steam gasification of biomass with in situ CO2 absorption in a dual fluidized bed system of 8 MW fuel input. Fuel Processing Technology, 90(7-8), 914-921.

[54] Wilk, V., Hofbauer, H. (2013). Conversion of mixed plastic wastes in a dual fluidized bed steam gasifier. Fuel, 107, 787-799.

[55] Molino, A., Chianese, S., Musmarra, D. (2016). Biomass gasification technology: The state of the art overview. Journal of Energy Chemistry, 25(1), 10-25.

[56] Quaak, P., Knoef, H., Stassen, H. (1999). Energy from biomass: a review of combustion and gasification technologies. The World Bank.

[57] Sansaniwal, S. K., Pal, K., Rosen, M. A., Tyagi, S. K. (2017). Recent advances in the development of biomass gasification technology: A comprehensive review. Renewable and Sustainable Energy Reviews, 72, 363-384.

[58] Skrzypkiewicz, M., Wierzbicki, M., Stępień, M. (2016). Solid Oxide Fuel Cells coupled with a biomass gasification unit. In E3S Web of Conferences (Vol. 10, p. 00115). EDP Sciences.

[59] Hrbek, J. (2016). Status report on thermal biomass gasification in countries participating in IEA Bioenergy Task 33.

[60] Ridjan, I., Mathiesen, B. V., Connolly, D. (2013). A review of biomass gasification technologies in Denmark and Sweden. Aalborg University Department of Development and Planning, Aalborg.

[61] Molino, A., Larocca, V., Chianese, S., Musmarra, D. (2018). Biofuels production by biomass gasification: A review. Energies, 11(4), 811.

[62] Burra, K. G., Gupta, A. K. (2018). Synergistic effects in steam gasification of combined biomass and plastic waste mixtures. Applied Energy, 211, 230-236.

[63] Zhou, H., Meng, A., Long, Y., Li, Q., Zhang, Y. (2014). Classification and comparison of municipal solid waste based on thermochemical characteristics. Journal of the Air Waste Management Association, 64(5), 597-616.

[64] Marinkovic, J. (2015). Use of Bed Materials in Dual Fluidized Bed (DFB) Systems (Doctoral dissertation, Chalmers University of Technology).

[65] Mastellone, M. L., Arena, U. (2008). Olivine as a tar removal catalyst during fluidized bed gasification of plastic waste. AIChE Journal, 54(6), 1656-1667.

[66] Vilches, TB. (2018).Operational strategies to control the gas composition in dual fluidized bed biomass gasifiers (Doctoral dissertation, Chalmers University of Technology).

[67] Thermal analysis of polymers, selected application. Mettler Toledo. https://www.mt.com/dam/LabDiv/guides-glen/ta-polymer/TA Polymers Selected AppsEN.pdf

[68] TGA701 Thermogravimetric Analyzer, LECO.http://leco-korea.com /wi_files/itemwi_pdf/15wi_69.pdf.

[69] TGA 701 Thermogravimetric Analyzer Specification Sheet. http://www.alpha-pribor.com.ua/pdf/TGA-701_Spec.pdf

[70] Ouyang, F., Levenspiel, O. (1986). Spiral distributor for fluidized beds. Industrial Engineering Chemistry Process Design and Development, 25(2), 504-507.

[71] Stenberg, V., Rydén, M., Mattisson, T., Lyngfelt, A. (2018). Combustion of methane in a bubbling fluidized bed with oxygen carrier aided combustion. 23rd International Conference on FBC. 927-936.

[72] Zhang, Y. M., Lu, C. X., Shi, M. X. (2008). A practical method to estimate the bed height of a fluidized bed of fine particles. Chemical Engineering Technology: Industrial Chemistry-Plant Equipment-Process Engineering-Biotechnology, 31(12), 1735-1742.

[73] Israelsson, M., Seemann, M., Thunman, H. (2013). Assessment of the solid-phase adsorption method for sampling biomass-derived tar in industrial environments. Energy Fuels, 27(12), 7569-7578.

[74] Meng, A., Chen, S., Long, Y., Zhou, H., Zhang, Y., Li, Q. (2015). Pyrolysis and gasification of typical components in wastes with macro-TGA. Waste management, 46, 247-256.

[75] Yang, T., Hu, K., Li, R., Sun, Y., Kai, X. (2015). Cogasification of typical plastics and rice straw with carbon dioxide. Environmental Progress Sustainable Energy, 34(3), 789-794.

[76] Rostek, E., Biernat, K. (2013). Thermogravimetry as a Research Method in the Transformation Processes of Waste Rubber and Plastic Products for Energy Car-

riers (WtE and WtL Processes). Journal of Sustainable Development of Energy, Water and Environment Systems, 1(2), 163-171.

[77] Sánchez, M., Morán, A., Escapa, A., Calvo, L., Martínez, O. (2007). Simultaneous thermogravimetric and mass spectrometric analysis of the pyrolysis of municipal solid wastes and polyethylene terephthalate. Journal of Thermal Analysis and Calorimetry, 90(1), 209-215.

[78] Dimitrov, N., Krehula, L. K., Siročić, A. P., Hrnjak-Murgić, Z. (2013). Analysis of recycled PET bottles products by pyrolysis-gas chromatography. Polymer degradation and stability, 98(5), 972-979.

[79] Horton, S. R., Woeckener, J., Mohr, R., Zhang, Y., Petrocelli, F., Klein, M. T. (2015). Molecular-level kinetic modeling of the gasification of common plastics. Energy Fuels, 30(3), 1662-1674.

[80] Luo, J., Li, Q., Meng, A., Long, Y., Zhang, Y. (2018). Combustion characteristics of typical model components in solid waste on a macro-TGA. Journal of Thermal Analysis and Calorimetry, 132(1), 553-562.

[81] Moltó, J., Font, R., Conesa, J. A. (2007). Kinetic model of the decomposition of a PET fibre cloth in an inert and air environment. Journal of analytical and applied pyrolysis, 79(1-2), 289-296.

[82] Silvarrey, L. D., Phan, A. N. (2016). Kinetic study of municipal plastic waste. International journal of hydrogen energy, 41(37), 16352-16364.

[83] Mastral, F. J., Esperanza, E., Garcıa, P., Juste, M. (2002). Pyrolysis of high-density polyethylene in a fluidised bed reactor. Influence of the temperature and residence time. Journal of Analytical and Applied Pyrolysis, 63(1), 1-15.

[84] Lars, W. Torbjörn,N HEATING VALUE OF GASES FROM BIOMASS GASIFICATION Report prepared for: IEA Bioenergy Agreement,Task 20 - Thermal Gasification of Biomass.

[85] Lee, U., Chung, J. N., Ingley, H. A. (2014). High-temperature steam gasification of municipal solid waste, rubber, plastic and wood. Energy Fuels, 28(7), 4573-4587.

[86] Brown, C. E. (2012). Applied multivariate statistics in geohydrology and related sciences. Springer Science Business Media, 155.

[87] Burra, K. G., Gupta, A. K. (2018). Synergistic effects in steam gasification of combined biomass and plastic waste mixtures. Applied energy, 211, 230-236.

A

Particle size

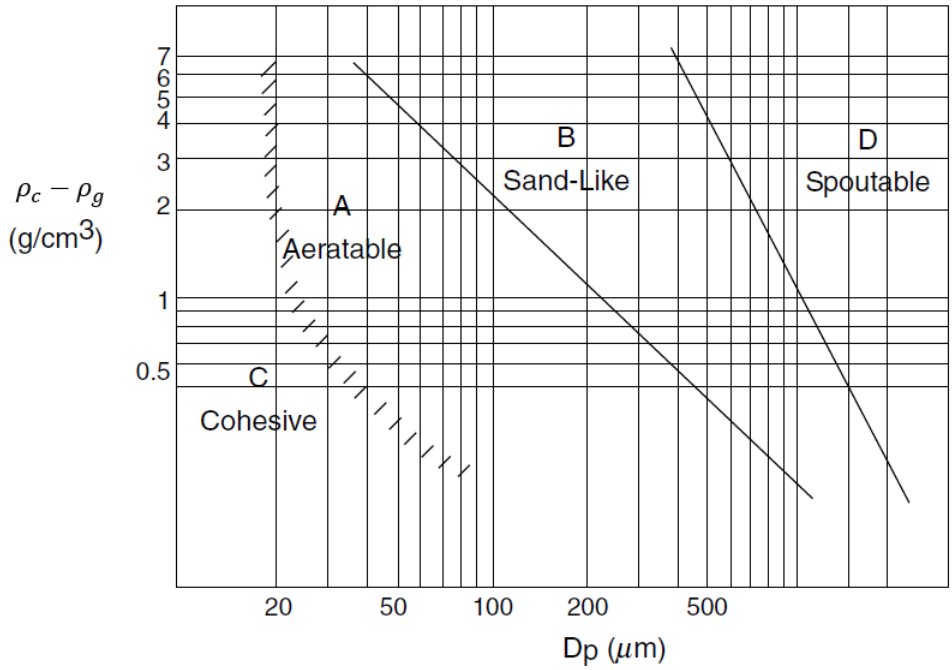

Figure A.1: Powder classification developed by Geldart [43]

B

TGA results of VPET, RPET, PE and the influence of bed material at 10, 20 and 30 $°C/min$

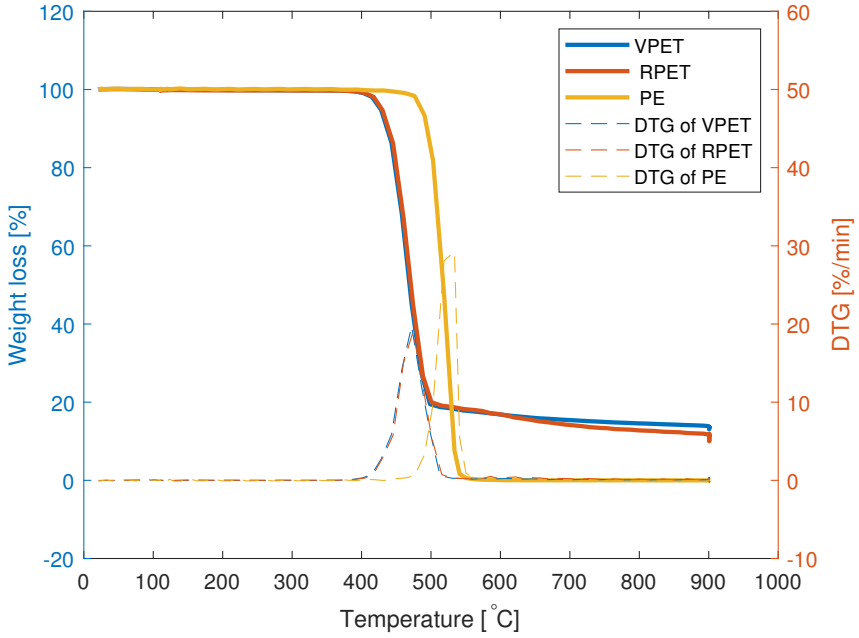

Figure B.1: TGA of VPET, RPET and PE at 10$°C/min$

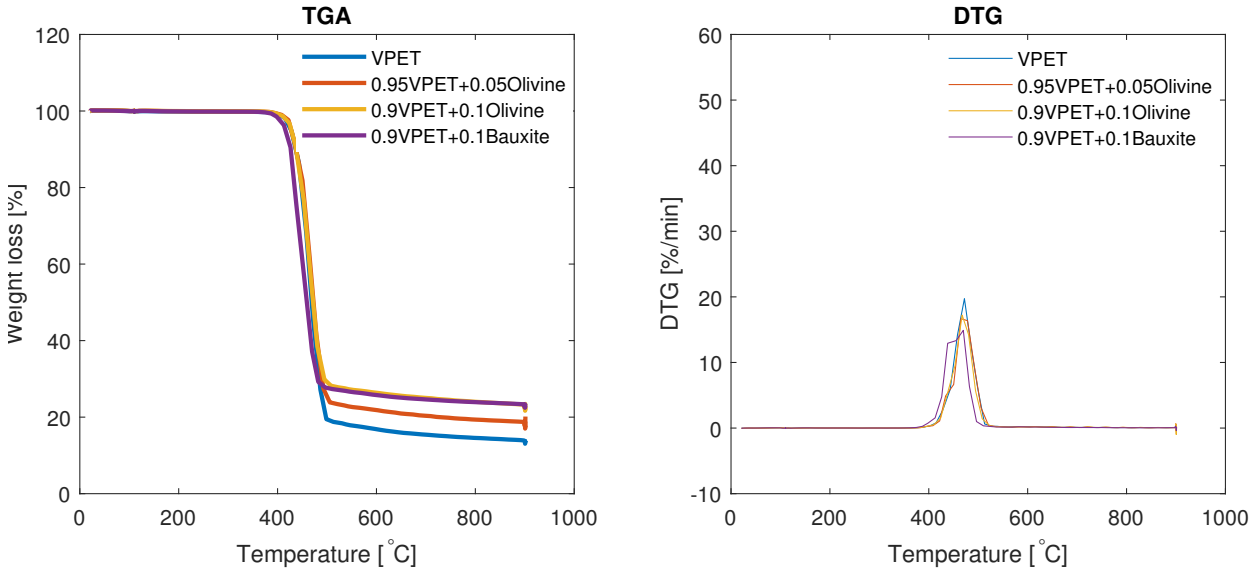

Figure B.2: The influence of bed material on VPET pyrolysis at $10°C/min$

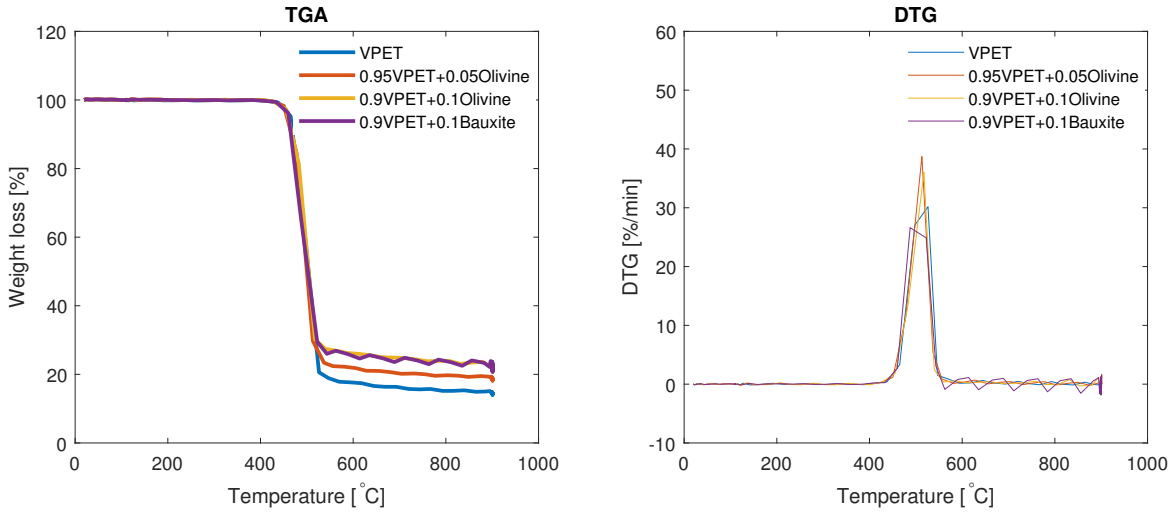

Figure B.3: The influence of bed material on VPET pyrolysis at $20°C/min$

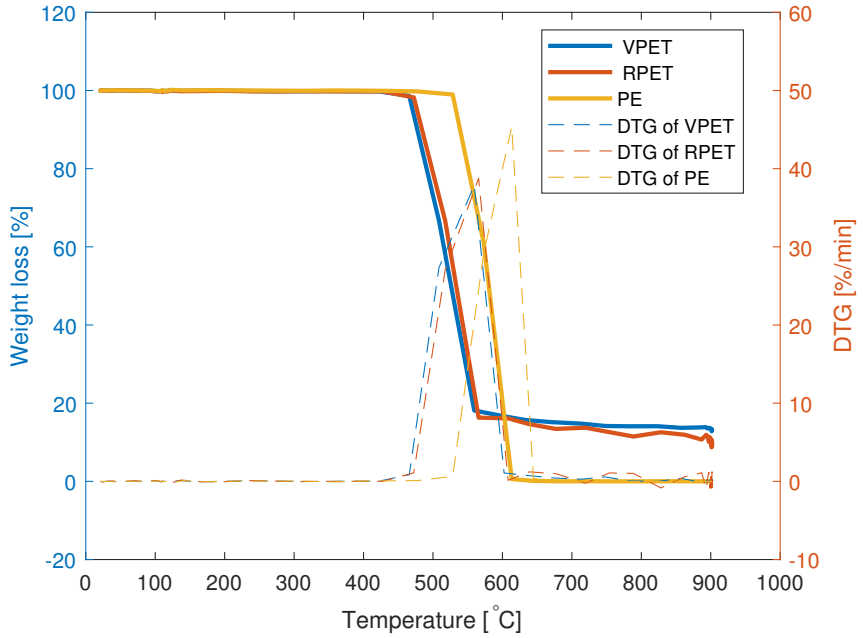

Figure B.4: TGA of VPET, RPET and PE at 30$°C/min$

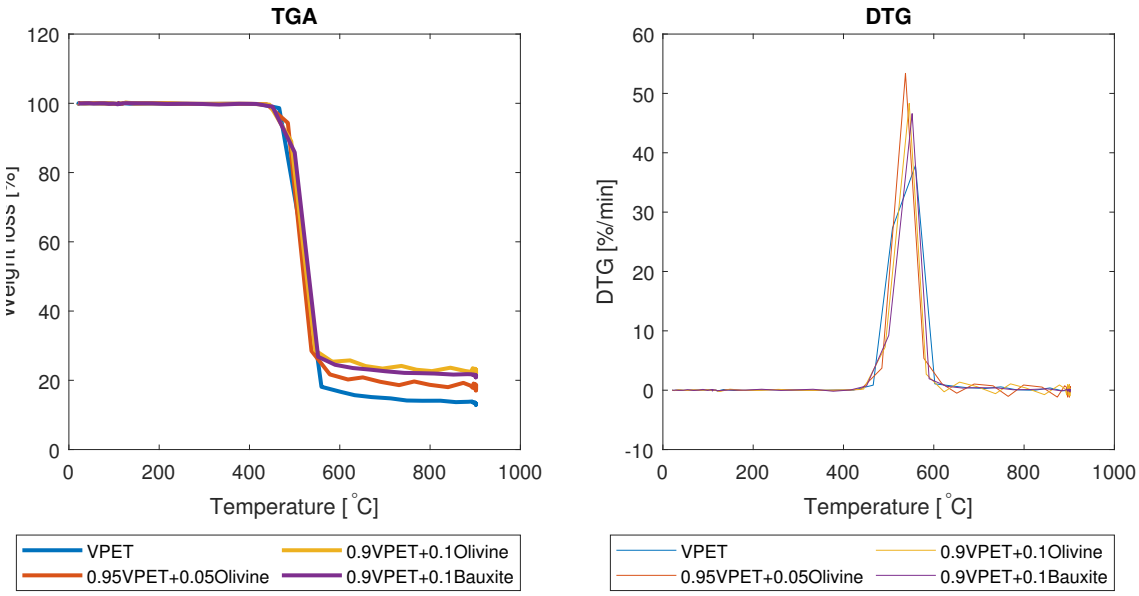

Figure B.5: The influence of bed material on VPET pyrolysis at 30$°C/min$

C

TGA results of proximate analysis at 10, 20 and 30 $^{\circ}C/min$

Table C.1: TGA results of proximate analysis at 10,20 and 30 $^{\circ}C/min$ (wt%)

Heating value	Feedstock	Moisture	Volatiles	Ash	Fixed carbon
10	RPET	0.22	88.18	0	11.62
	0.95VPET+0.05Olivine	0.03	81.98	4.24	13.75
	0.9VPET+0.1Olivine	0.01	77.65	9.24	13.10
	0.9VPET+0.1Bauxite	0.02	77.30	8.54	14.14
20	0.95VPET+0.05Olivine	0.02	81.68	4.38	14.04
	0.9VPET+0.1Olivine	0.03	78.45	7.96	13.56
	0.9VPET+0.1Bauxite	0.02	77.87	9.12	13.00
30	RPET	0.21	90.44	0.02	9.33
	PE	0.05	99.94	0	0.01
	0.95VPET+0.05Olivine	0.10	82.27	4.71	12.92
	0.9VPET+0.1Olivine	0.11	77.86	8.75	13.29
	0.9VPET+0.1Bauxite	0.14	78.89	9.14	11.83

Note: Due to the rounding, the total of each composition may not be 1

D

Summary of syngas application evaluation

Table D.1: Summary of syngas application evaluation

Plastic	Agent	Temperature(°C)	Residence time (s)	S/F	CGEE (no tar)	CGEE (with tar)	tar (mg/Nm^3)	Possible products/processes
PE	N_2	750	3.23	-	69.6%	-	-	FTS
PE	Steam	750	3.23	2	57.1%	-	-	H_2 SNG
VPET	N_2	750	3.23	-	7.3%	-	-	-
-								
VPET	Steam +air	750	3.23	-	10.6%	-	-	DME FTS
VPET	Air	750	3.23	-	20.3%	-	-	- Ethanol
VPET	Steam	750	3.23	2	13.4%	-	-	DME FTS
RPET	N_2	750	3.23	-	14.8%	-	-	-
RPET	Steam	750	3.23	2	15.0%	-	-	FTS
28.7%								
VPET	Steam	750	3.23	1.25	24.2%	51.2%	135.3	FTS
VPET	Steam	750	3.23	2.5	23.3%	50.0%	149.9	FTS
VPET	Steam	750	3.23	3.75	21.5%	49.8%	170.5	FTS Ethanol
11.5%								
VPET	Steam	700	3.23	2.5	10.8%	57.6%	249.2	FTS
VPET	Steam	800	3.23	2.5	31%	53.4%	137.6	FTS
VPET	Steam	750	4.03	2.5	20.6%	48.7%	196.3	FTS Ethanol
VPET	Steam	750	4.83	2.5	21.2%	51.9%	160.4	FTS

E

Detailed tar distribution at different temperatures

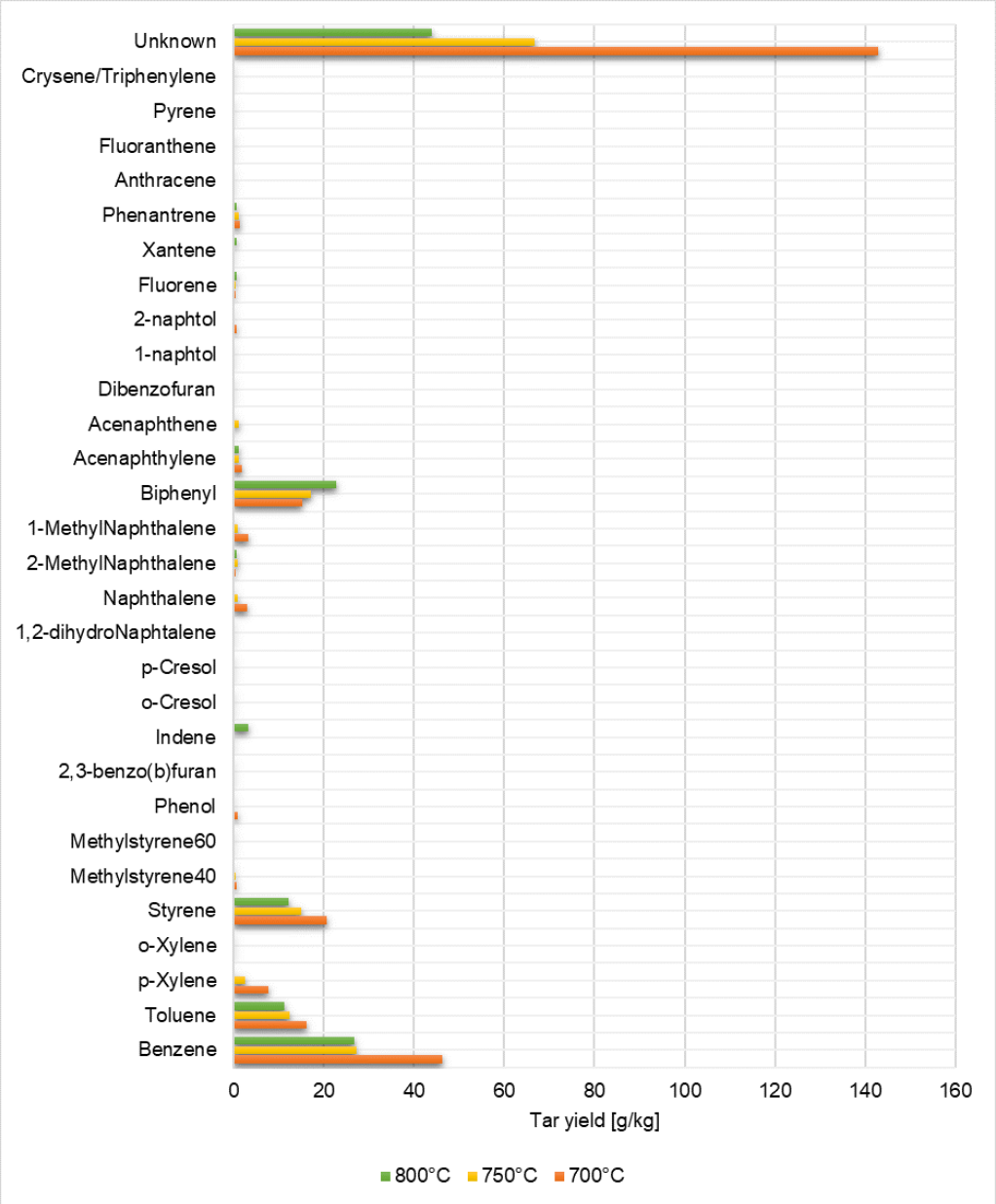

Figure E.1: Detailed tar distribution at different temperatures